Introduction à la physique des décharges impulsionnelles (Partie 1)

David Z. Pai

Chargé de recherche

Axe Electrofluidodynamique
Département Fluides, Thermique et Combustion

Institut P' • UPR CNRS 3346
SP2MI • Téléport 2
Boulevard Marie et Pierre Curie • BP 30179
F86962 FUTUROSCOPE CHASSENEUIL Cedex

La première décharge impulsionnelle ?

NOTES

ON

RECENT RESEARCHES IN

ELECTRICITY AND MAGNETISM

INTENDED AS A SEQUEL TO

PROFESSOR CLERK-MAXWELL'S TREATISE
ON ELECTRICITY AND MAGNETISM

BY

J. J. THOMSON, M.A., F.R.S.
HON. SC.D. DUBLIN
FELLOW OF TRINITY COLLEGE
PROFESSOR OF EXPERIMENTAL PHYSICS IN THE UNIVERSITY OF CAMBRIDGE

Oxford
AT THE CLARENDON PRESS
1893

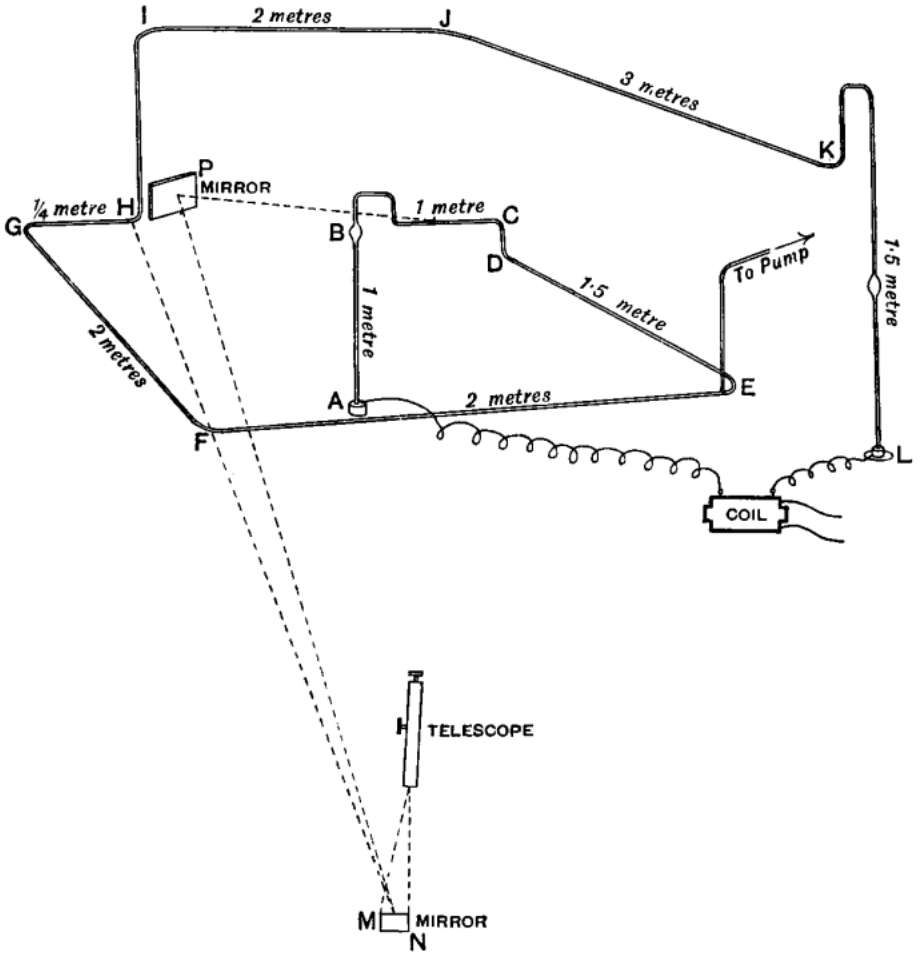

Fig. 42.

Historique de la recherche en décharges nanosecondes

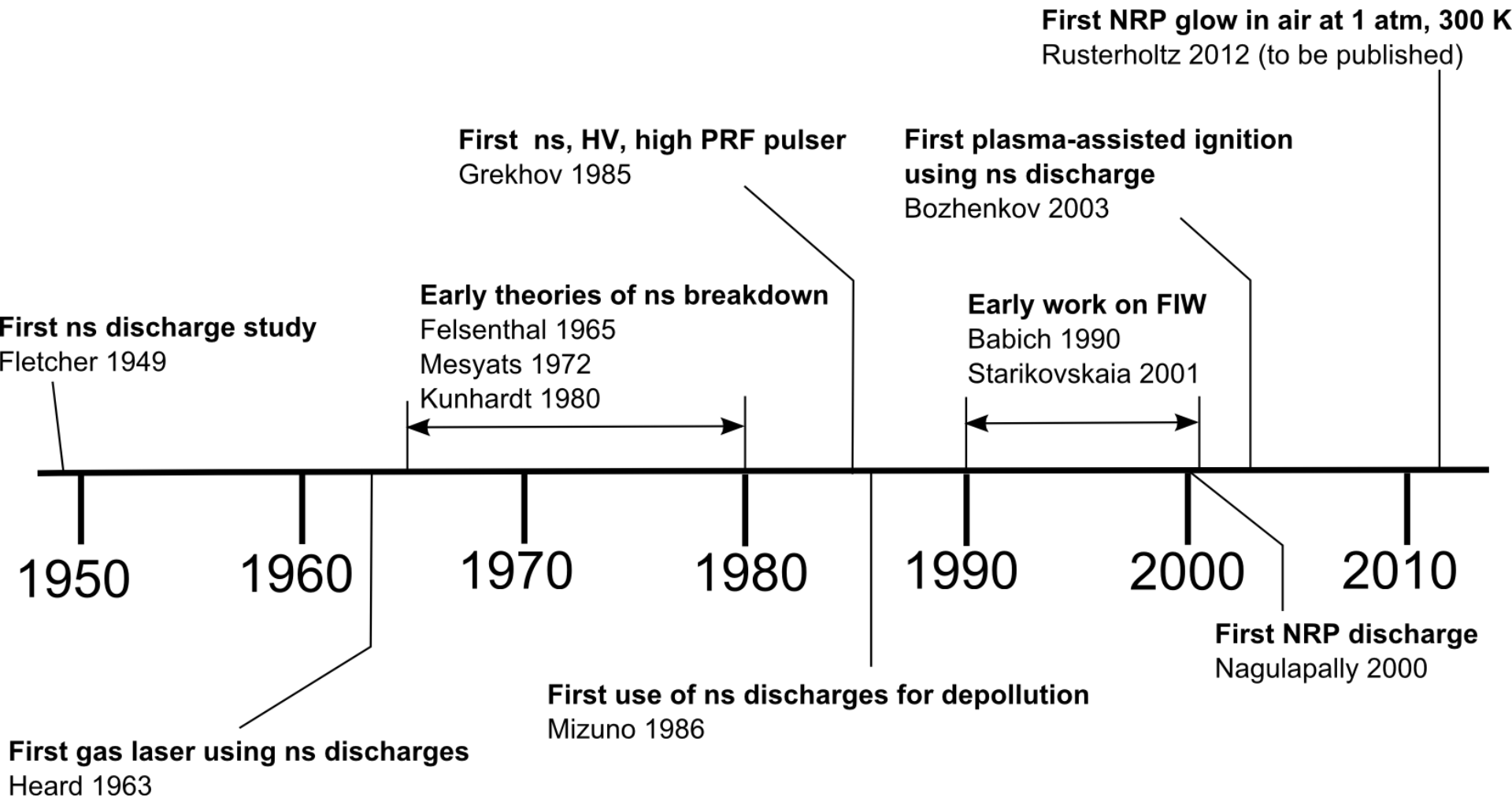

Bilan de la présentation

- Motivation pour l'utilisation des décharges impulsionnelles
- Propriétés plasmas : densité des électrons, température des électrons, champ électrique
- Dynamique des décharges : streamers, uniformité, région cathodique
- Régimes des décharges impulsionnelles

Conditions générales

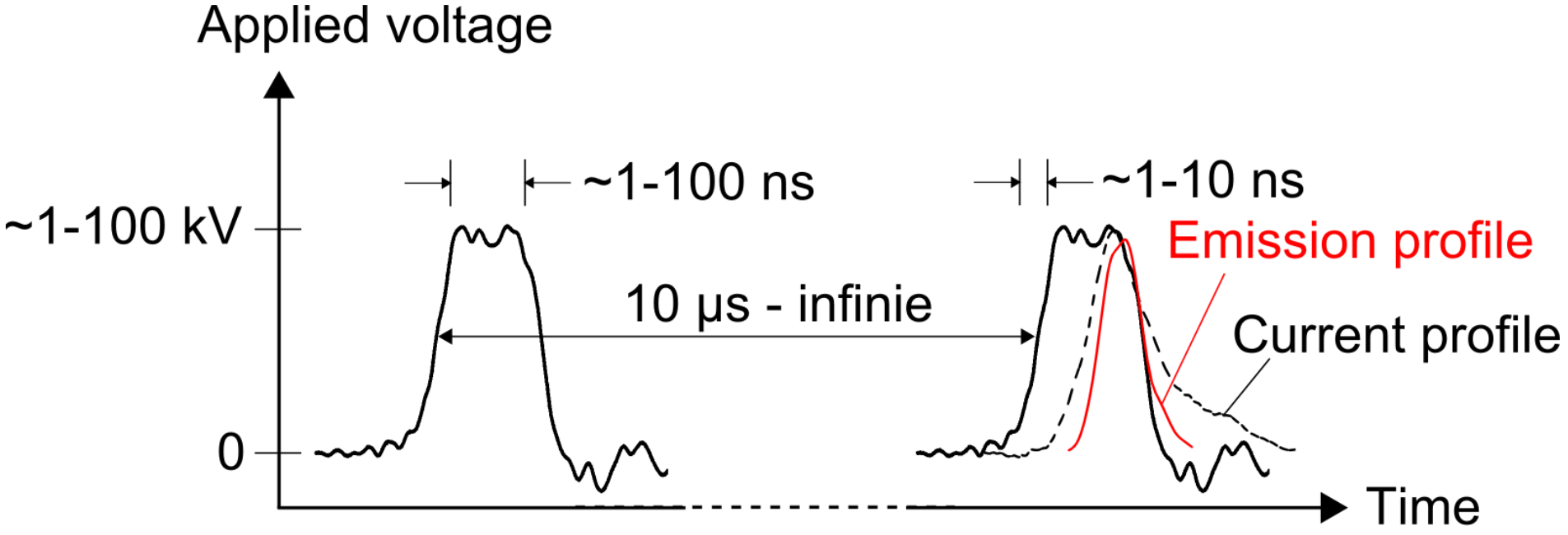

- Par défaut :
  - 1 atm
  - Air
  - Géométrie pointe-pointe ou pointe-plan (~1 – 10 mm)

POURQUOI UTILISER LES DÉCHARGES IMPULSIONNELLES

Comparatif énergétique

Denis Packan, PhD Thesis, Stanford University, 2003

DC discharge

Gas temperature at nozzle exit: 2000 K
Nozzle diameter: 1.5 cm
Gas velocity: ~450 m/s
Discharge current: 150 mA
Discharge electric field: 1600 V/cm
Electrode gap: 3.5 cm (cathode at bottom)
Discharge diameter: ~3 mm
Electron density in discharge:~10^{12} cm^{-3}

Power dissipated in discharge: **3000 W/cm^3**

Repetitively pulsed discharge

Temperature at nozzle exit: 2000 K
Nozzle diameter: 7 cm
Gas velocity: ~10 m/s
Electrode gap: 1 cm (cathode at bottom)
Diameter discharge: ~3 mm
Pulsed electric field: 5300 V/cm
Pulsed current: ~850 mA
Pulse duration: 10 ns
Repetition rate: 30 kHz
Electron density (time average):~10^{12} cm^{-3}

Power dissipated in discharge: **10 W/cm^3**

Durée de l'impulsion

Hackam & Akiyama, IEEE DEI 2000

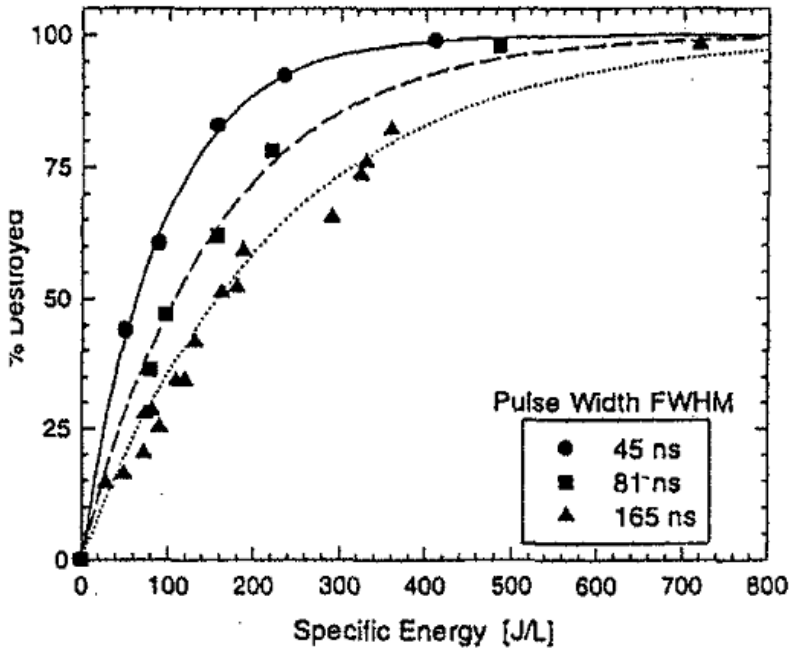

Figure 41. Destruction of toluene in air using different positive pulse widths in a coaxial corona discharge reactor. Pulse rise time and corresponding FWHM: 9 ns and 45 ns; 15 ns (81 ns); 25 ns (165 ns); concentration of toluene 200 ppm [94].

Ono et al, J Phys D 2011

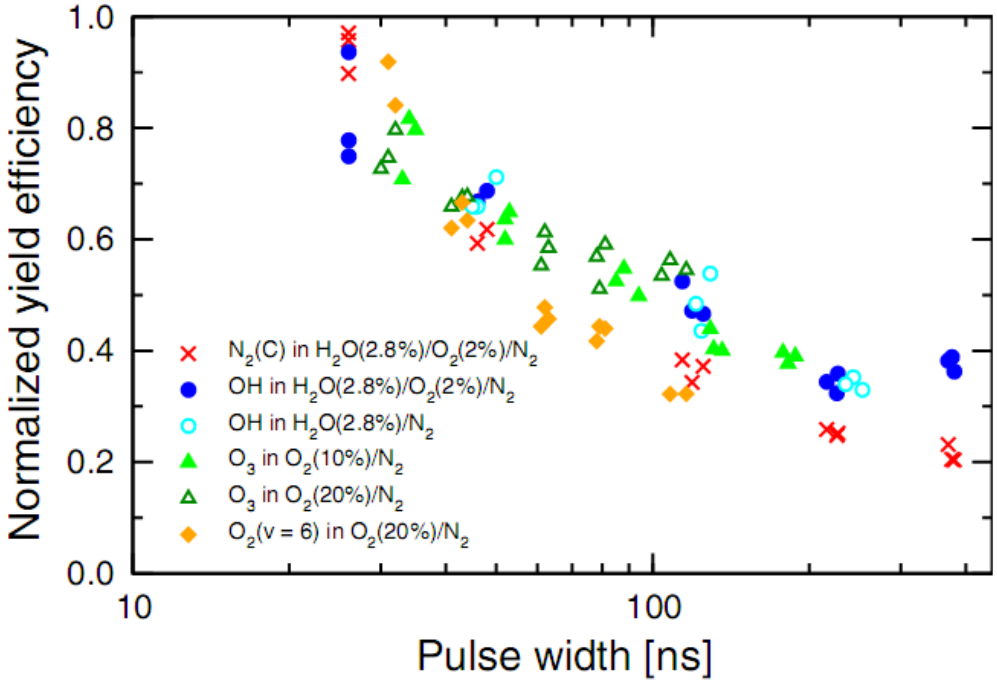

Figure 15. Normalized yield efficiency of various species as a function of discharge pulse width. O_3 is measured in 25 gaps and others are measured in single gap.

Temps de montée

Huiskamp et al, J Phys D 2017

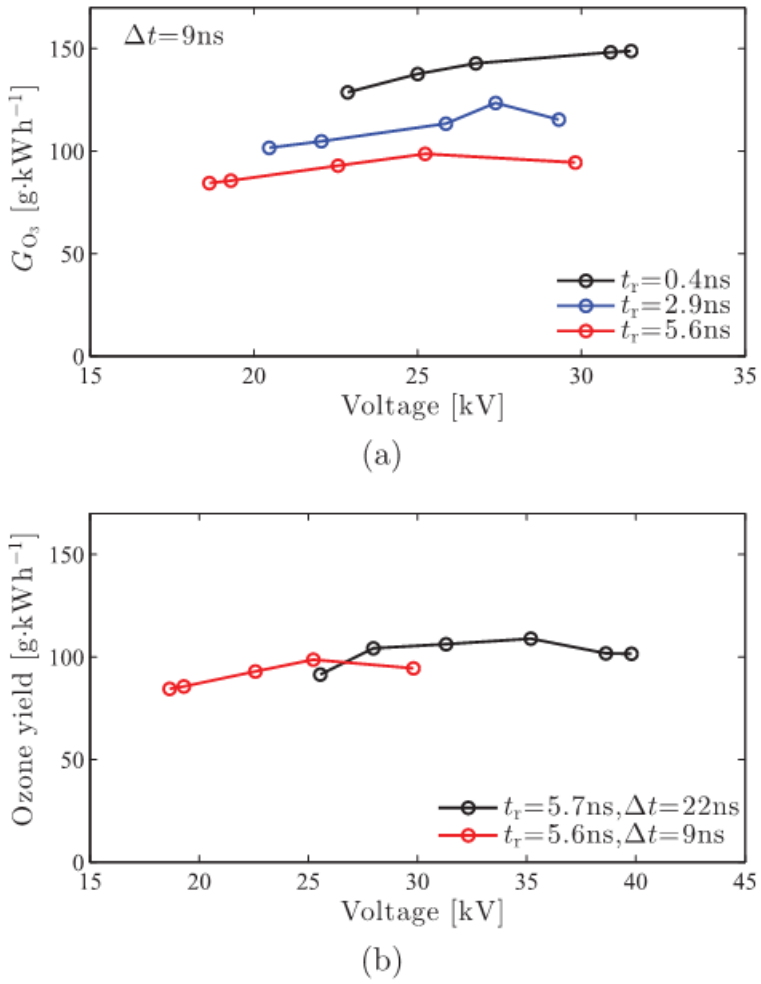

Figure 10. Ozone yields for pulses with different rise times. In (a) we used the pulses from the nanosecond pulse source with 9 ns pulse duration with three different rise times for $f_{rr} = 20$ Hz and $F = 2$ slm. In (b) we compared the ozone yield of the 5.6 ns rise time pulse of the nanosecond pulse source of (a) with the yield of the conventional pulse source. The experimental settings for the measurements with the conventional pulse source were the same as for (a).

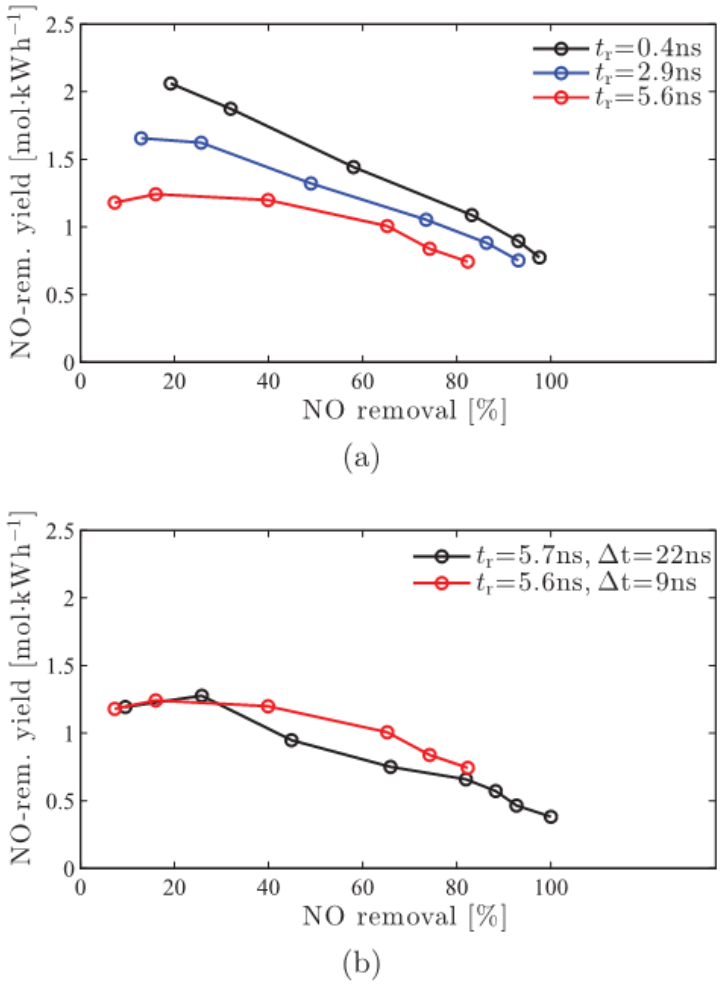

Figure 17. NO-removal yields for different rise-time pulses. In (a) all pulses were the 9 ns pulses from the nanosecond pulse source with a 30 kV amplitude and different rise times. The gas flow was 2 slm of synthetic air with 220 ppm NO. In (b) the NO-removal yields for the 5.6 ns rise time pulses from the nanosecond pulse source (same experimental conditions as (a)) are compared with NO-removal yields for the 5.7 ns rise time pulse from the conventional pulse source (38 kV pulses at $F = 2$ slm).

ns pulse

AC

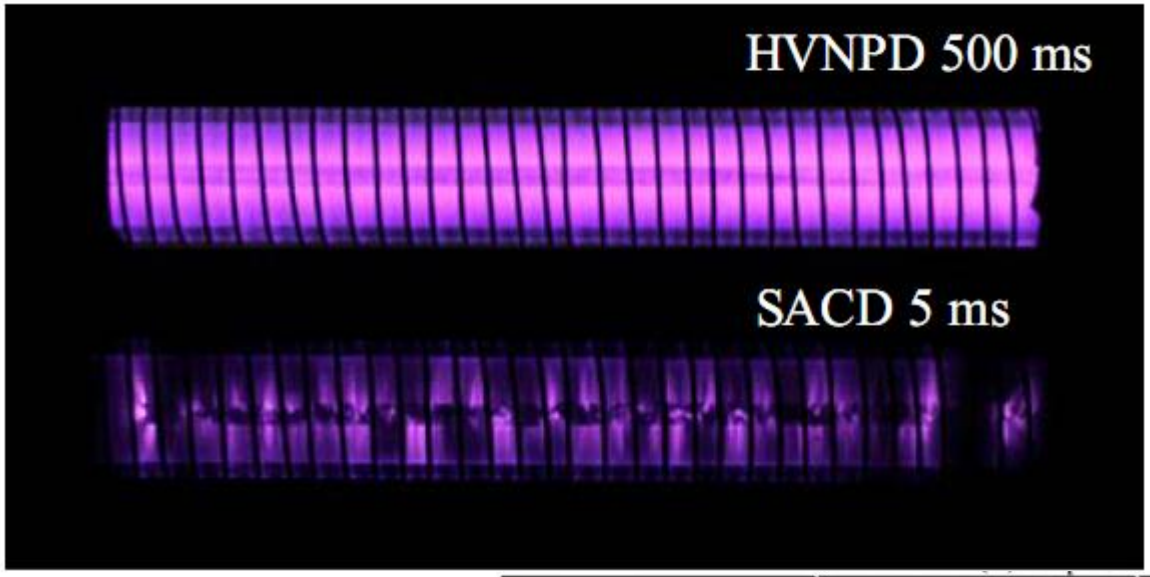

Zhang et al, JAP 2013

µs pulse

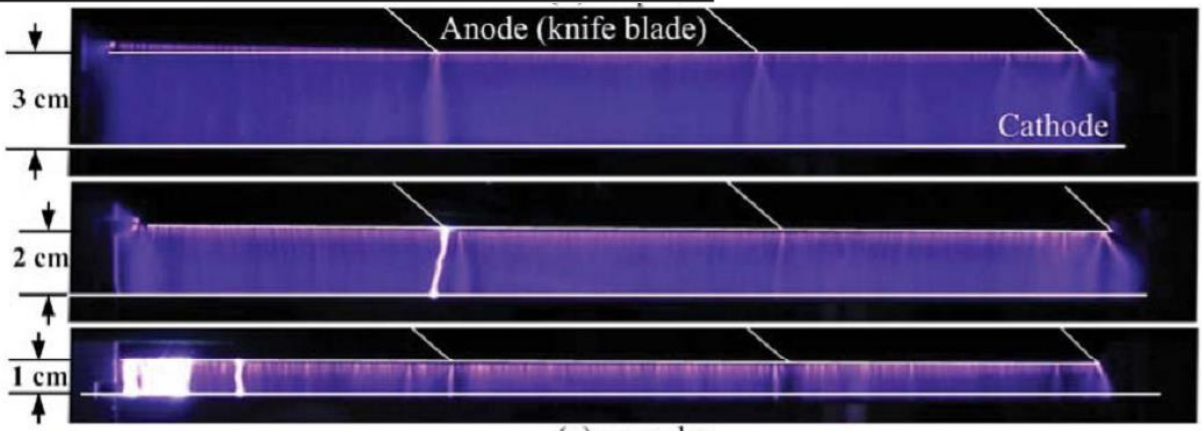

(c) µs-pulse

Shao et al, IEEE TPS 2014

ns pulse

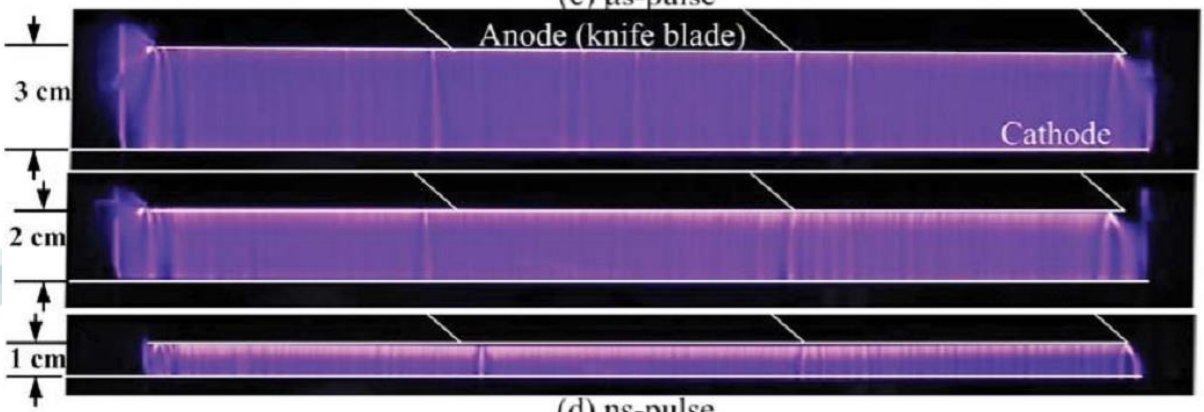

(d) ns-pulse

Pourquoi utiliser les décharges impulsionnelles ?

- Canaliser l'énergie de manière efficace
  - Augmenter la densité des espèces d'intérêt (ex. électrons, radicaux)
  - Eviter le réchauffement du gaz ou d'une surface
- Permettre un régime diffus/homogène
  - Eviter la transition vers l'arc ou les filaments
- Induire des effets thermiques, hydrodynamiques (Partie 2)

Efficacité énergétique à fort champ électrique

Raizer, « Gas Discharge Physics », 1991

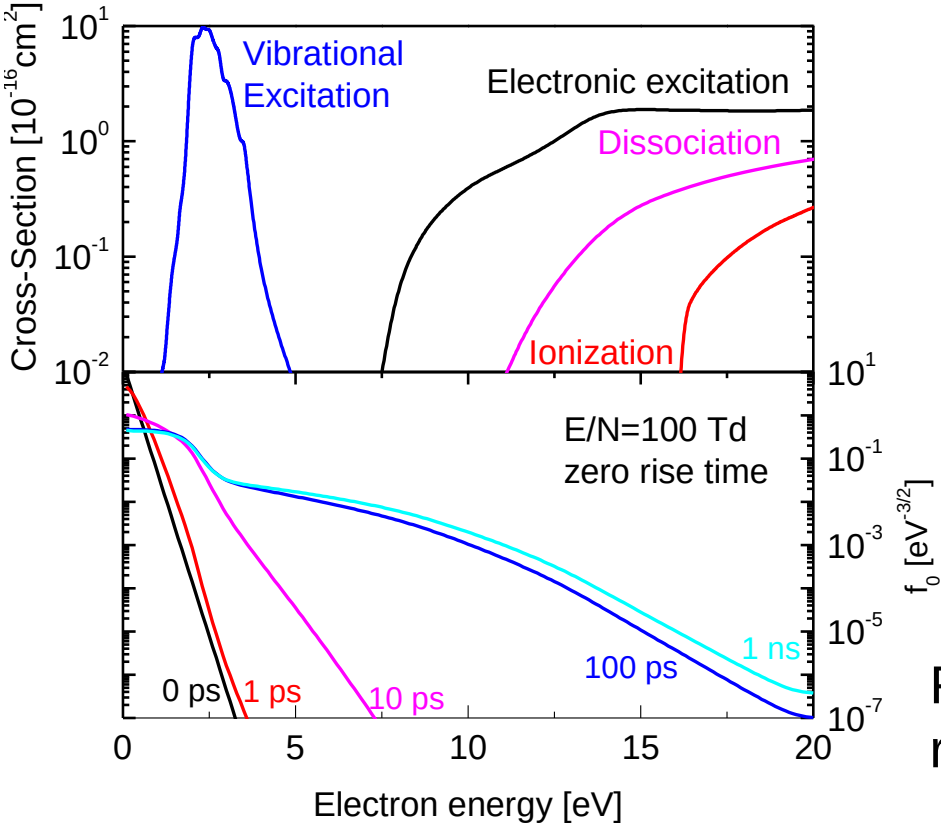

Aleksandrov et al, High Temp 1991
Nighan, Phys Rev A 1970

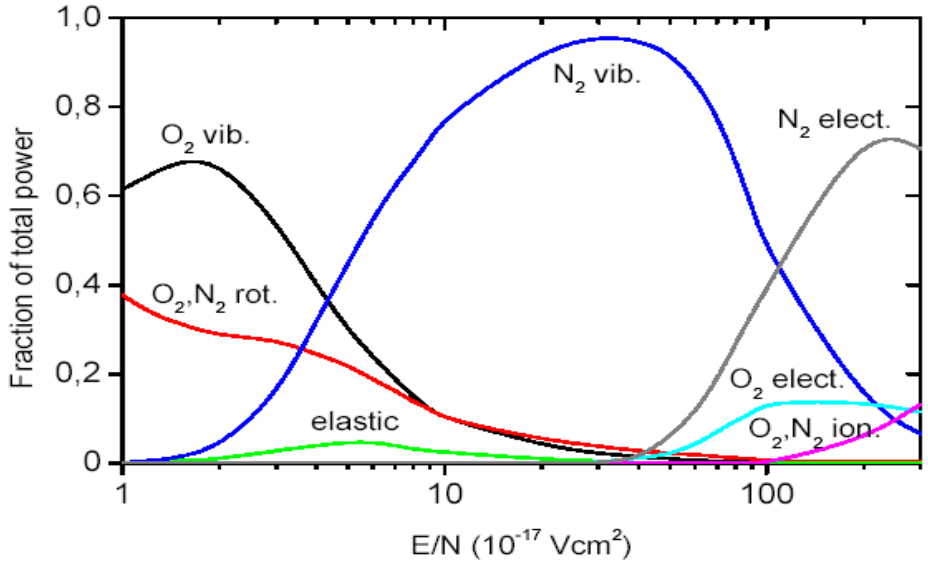

Fort champ électrique appliqué rapidement :

- Electrons à haute énergie favorisent excitation électronique, ionisation, dissociation
- Pertes minimisées
- Energie dirigée vers la chimie au lieu de la thermique

Echelles de temps

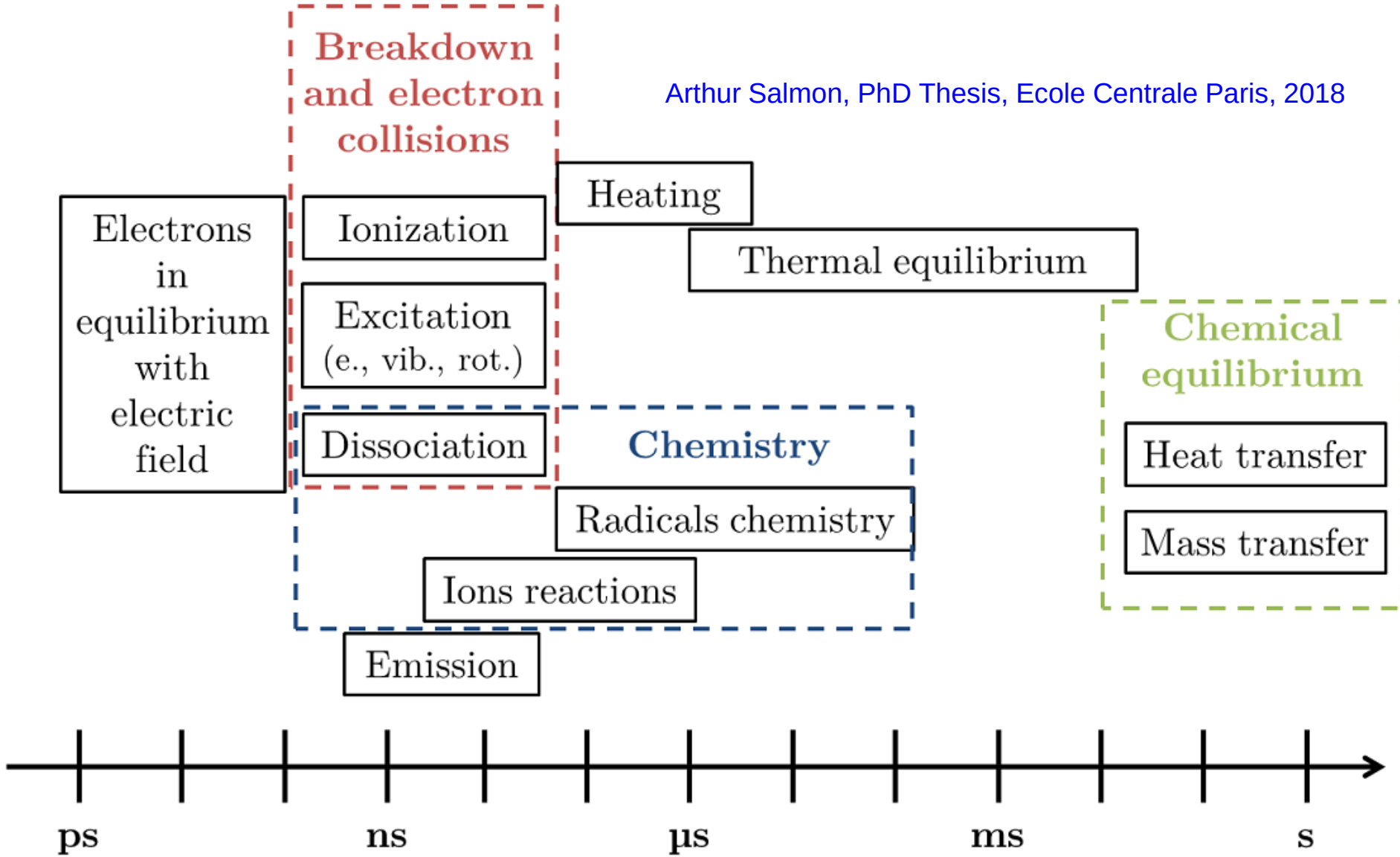

PROPRIETES PLASMAS : TRAITEMENT 0-D

Temps caractéristiques

Table 9.1. Time scales of various discharge processes under conditions typical of discharge in cw CO_2 lasers ($CO_2 + N_2 + He$); $p \sim 10$–100 Torr, $N \sim 10^{18}\,10^{-3}$, $T \sim 300$–500 K, $E/p \sim 10$ V/(cm·Torr), $T_e \approx 1$ eV, $T_V \approx 2000$–5000 K, $n_e \sim 10^{10}$ cm^{-3}, $\Lambda \sim 1$ cm [a)]

Process	Characteristic time	Duration, s
1. Space-charge relaxation	$\tau_\sigma = 1/4\pi\sigma$	10^{-10}–10^{-9}
2. Collisional energy transfer		
(1) electron tempeature relaxation	$\tau_u = 1/\nu_m\delta_1$	10^{-9}–10^{-8}
(2) gas heating	$\tau_T = Nc_{p1}T/\sigma E^2$	10^{-3}–10^{-2}
(3) pumping of molecular vibrations	$\tau_V = N_M c_V T_V/\sigma E^2$	10^{-3}–10^{-2}
(4) vibrational relaxation	τ_{VT}	10^{-4}–10^{-2}
3. Collision kinetics		
(1) ionization	$\tau_i = (k_i N)^{-1}$	10^{-5}–10^{-4}
(2) attachment	$\tau_a = (k_a N)^{-1}$	10^{-6}–10^{-5}
(3) detachment	$\tau_d = (k_d N)^{-1}$	10^{-6}–10^{-5}
(4) electron excitation	$\tau^* = (k^* N)^{-1}$	10^{-6}–10^{-4}
(5) electron-ion recombination	$\tau_{rec}^e = (\beta_e n_+)^{-1}$	10^{-4}–10^{-3}
(6) ion-ion recombination	$\tau_{rec}^- = (\beta_- n_+)^{-1}$	10^{-4}–10^{-3}
4. Transport processes		
(1) pressure levelling (sound)	$\tau_s = \Lambda/c_s$	10^{-5}–10^{-4}
(2) heat conduction of the gas	$\tau_\chi = \Lambda^2/\chi$	10^{-2}
(3) ambipolar diffusion	$\tau_{da} = \Lambda^2/D_a$	10^{-2}
(4) electron heat conduction	$\tau_\chi^e = \Lambda^2/\chi_e$	10^{-5}

Raizer, « Gas Discharge Physics », 1991

Temps caractéristiques

Table 9.1. Time scales of various discharge processes under conditions typical of discharge in cw CO_2 lasers ($CO_2 + N_2 + He$); $p \sim 10$–100 Torr, $N \sim 10^{18}\,10^{-3}$, $T \sim 300$–500 K, $E/p \sim 10$ V/(cm·Torr), $T_e \approx 1$ eV, $T_V \approx 2000$–5000 K, $n_e \sim 10^{10}$ cm^{-3}, $\Lambda \sim 1$ cm [a)]

Process	Characteristic time	Duration, s
1. Space-charge relaxation	$\tau_\sigma = 1/4\pi\sigma$	10^{-10}–10^{-9}
2. Collisional energy transfer		
(1) electron tempeature relaxation	$\tau_u = 1/\nu_m\delta_1$	10^{-9}–10^{-8}
(2) gas heating	$\tau_T = Nc_{p1}T/\sigma E^2$	10^{-3}–10^{-2}
(3) pumping of molecular vibrations	$\tau_V = N_M c_V T_V/\sigma E^2$	10^{-3}–10^{-2}
(4) vibrational relaxation	τ_{VT}	10^{-4}–10^{-2}
3. Collision kinetics		
(1) ionization	$\tau_i = (k_i N)^{-1}$	10^{-5}–10^{-4}
(2) attachment	$\tau_a = (k_a N)^{-1}$	10^{-6}–10^{-5}
(3) detachment	$\tau_d = (k_d N)^{-1}$	10^{-6}–10^{-5}
(4) electron excitation	$\tau^* = (k^* N)^{-1}$	10^{-6}–10^{-4}
(5) electron-ion recombination	$\tau_{rec}^e = (\beta_e n_+)^{-1}$	10^{-4}–10^{-3}
(6) ion-ion recombination	$\tau_{rec}^- = (\beta_- n_+)^{-1}$	10^{-4}–10^{-3}
4. Transport processes		
(1) pressure levelling (sound)	$\tau_s = \Lambda/c_s$	10^{-5}–10^{-4}
(2) heat conduction of the gas	$\tau_\chi = \Lambda^2/\chi$	10^{-2}
(3) ambipolar diffusion	$\tau_{da} = \Lambda^2/D_a$	10^{-2}
(4) electron heat conduction	$\tau_\chi^e = \Lambda^2/\chi_e$	10^{-5}

Raizer, « Gas Discharge Physics », 1991

Deux exemples :

1) Faiblement ionisé
2) Fortement ionisé

Exemple faiblement ionisé dans le CO

Pietanza et al, JPP 2017

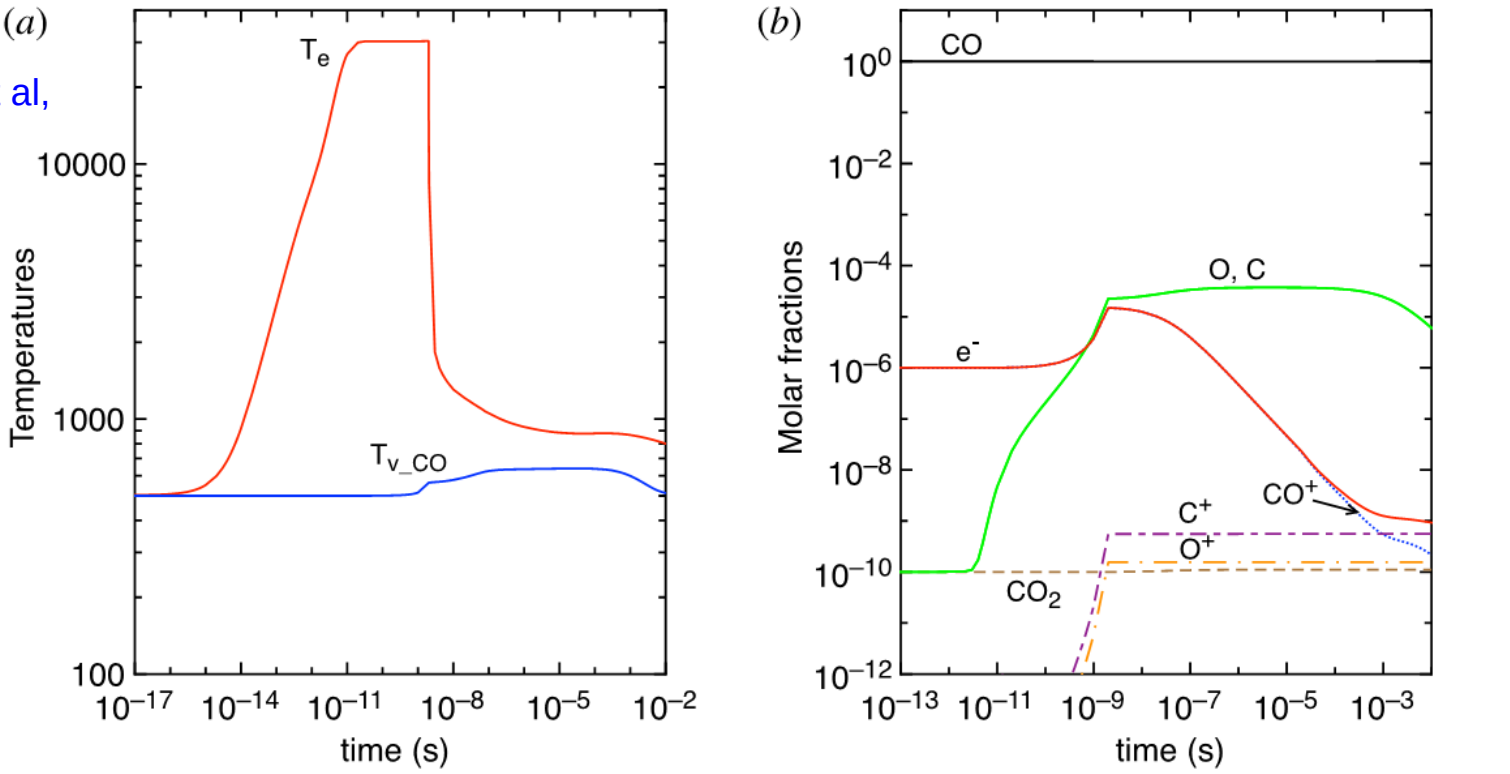

FIGURE 2. (*a*) Temperature and (*b*) molar fraction time evolution in case study 1 ($T_{gas} = 500$ K, $p = 1$ atm, E/N = 200 Td, $\tau_{pulse} = 2$ ns, $\tau_{afterglow} = 10$ ms).

$\tau_{EEDF} = (n_{CO}K^{1,0}_{eV})^{-1}$	$\tau_{e-V} = (n_e K^{1,0}_{eV})^{-1}$	$\tau_{V-V} = (n_{CO}K^{1,0}_{1,0})^{-1}$	$\tau_{V-T(CO)} = (n_{CO}K^{1,0}_{vT(CO)})^{-1}$	$\tau_{V-T(C,O)} = (n_C K^{1,0}_{vT(C,O)})^{-1}$
4.80×10^{-12} s	3.22×10^{-7} s	4.37×10^{-8} s	5.56×10^{-2} s	3.50×10^{-7} s

TABLE 2. Characteristic times evaluated at the end of the pulse ($\tau_{pulse} = 2$ ns) when the electron density is approximatley 2.2×10^{14} cm^{-3}.

Coefficient de perte par collision électronique

Bilan de l'énergie gagnée par le champ et perdue par collisions :

$$\frac{d\varepsilon}{dt} = eE\mathrm{v}_d - \delta_l \varepsilon \nu_m$$

Mitchner & Kruger, "Partially Ionized Gases", 1973

Électron-atome neutre (M & K p. 51) :

$$\Delta\varepsilon = \delta_l \varepsilon = \left(2m_e/m_h\right)\varepsilon$$

Electron-ion (M & K p. 51):

$$\Delta\varepsilon = \delta_l \varepsilon = \left(2m_e/m_h\right)\underbrace{\left(2\sin^2\frac{\chi}{2}\right)}_{\approx 1}\varepsilon$$

Electron-molécule (M & K p. 61)

$$\Delta\varepsilon = \delta_l \varepsilon = \left(2m_e/m_h\right)\delta_h \varepsilon$$

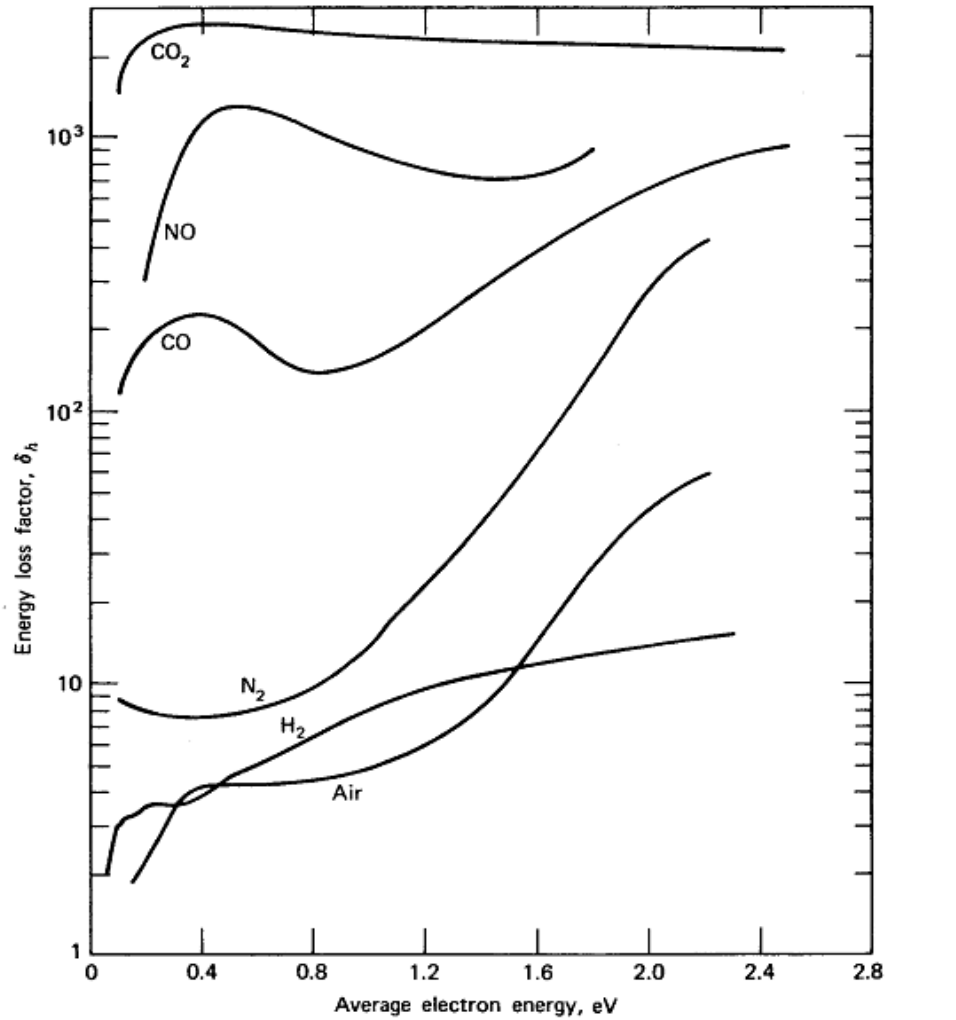

Figure 10. Energy loss of electrons in collisions with various molecular species (after Sutton and Sherman, 1965, p. 148).

Exemple faiblement ionisé dans le CO

Pietanza et al, JPP 2017

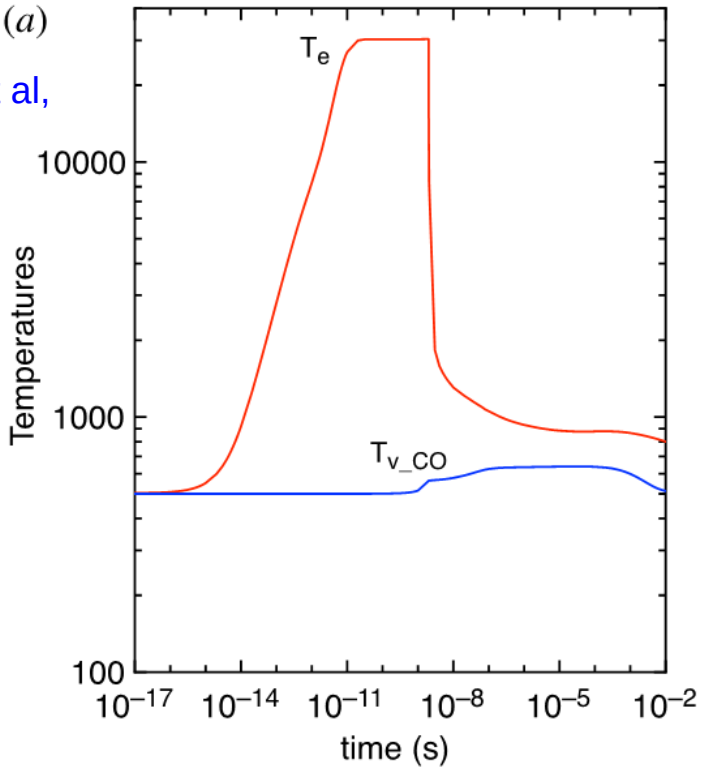

$$\nu_m = N\sigma_m\sqrt{8k_BT_e/\pi m_e} = 1.74 \text{ THz}$$

$$\delta_l = (2m_e/m_0)\delta_h = (2/1836/28)\cdot 1000 = 0.039$$

$$\tau_u = 1/\nu_m\delta_l = 1.5\times 10^{-11} \text{ s}$$

FIGURE 2. (*a*) Temperature and (*b*) molar fraction time evolution in case study 1 (T_{gas} = 500 K, p = 1 atm, E/N = 200 Td, τ_{pulse} = 2 ns, $\tau_{afterglow}$ = 10 ms).

$\tau_{EEDF} = (n_{CO}K_{eV}^{1,0})^{-1}$	$\tau_{e-V} = (n_eK_{eV}^{1,0})^{-1}$	$\tau_{V-V} = (n_{CO}K_{1,0}^{1,0})^{-1}$	$\tau_{V-T(CO)} = (n_{CO}K_{vT(CO)}^{1,0})^{-1}$	$\tau_{V-T(C,O)} = (n_CK_{vT(C,O)}^{1,0})^{-1}$
4.80×10^{-12} s	3.22×10^{-7} s	4.37×10^{-8} s	5.56×10^{-2} s	3.50×10^{-7} s

TABLE 2. Characteristic times evaluated at the end of the pulse (τ_{pulse} = 2 ns) when the electron density is approximatley 2.2×10^{14} cm^{-3}.

Exemple faiblement ionisé dans le CO

Pietanza et al, JPP 2017

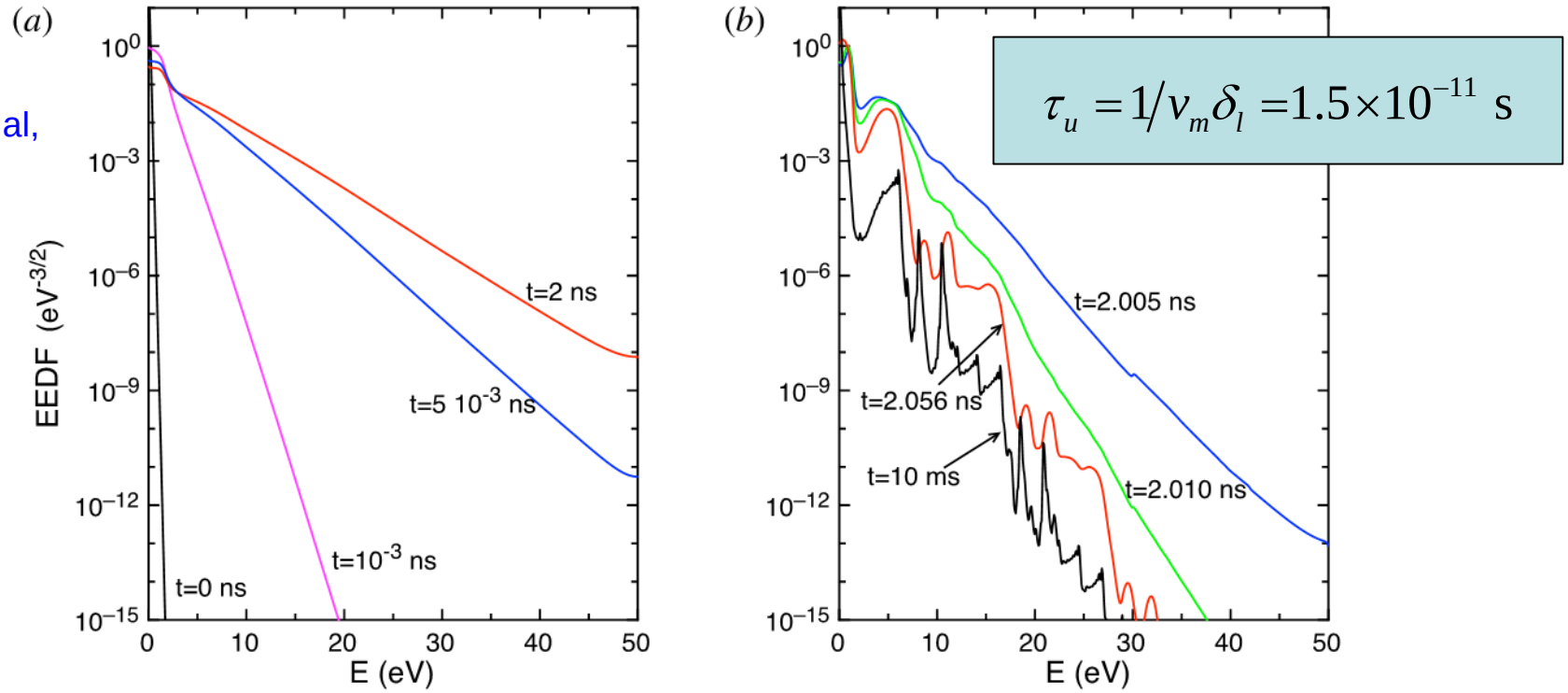

FIGURE 4. Electron energy distribution function in (*a*) discharge and (*b*) post-discharge conditions for case study 1 ($T_{gas} = 500$ K, $p = 1$ atm, E/N = 200 Td, $\tau_{pulse} = 2$ ns, $\tau_{afterglow} = 10$ ms).

$\tau_{EEDF} = (n_{CO} K^{1,0}_{eV})^{-1}$	$\tau_{e-V} = (n_e K^{1,0}_{eV})^{-1}$	$\tau_{V-V} = (n_{CO} K^{1,0}_{1,0})^{-1}$	$\tau_{V-T(CO)} = (n_{CO} K^{1,0}_{vT(CO)})^{-1}$	$\tau_{V-T(C,O)} = (n_C K^{1,0}_{vT(C,O)})^{-1}$
4.80×10^{-12} s	3.22×10^{-7} s	4.37×10^{-8} s	5.56×10^{-2} s	3.50×10^{-7} s

TABLE 2. Characteristic times evaluated at the end of the pulse ($\tau_{pulse} = 2$ ns) when the electron density is approximatley 2.2×10^{14} cm^{-3}.

Exemple faiblement ionisé dans le CO

Pietanza et al, JPP 2017

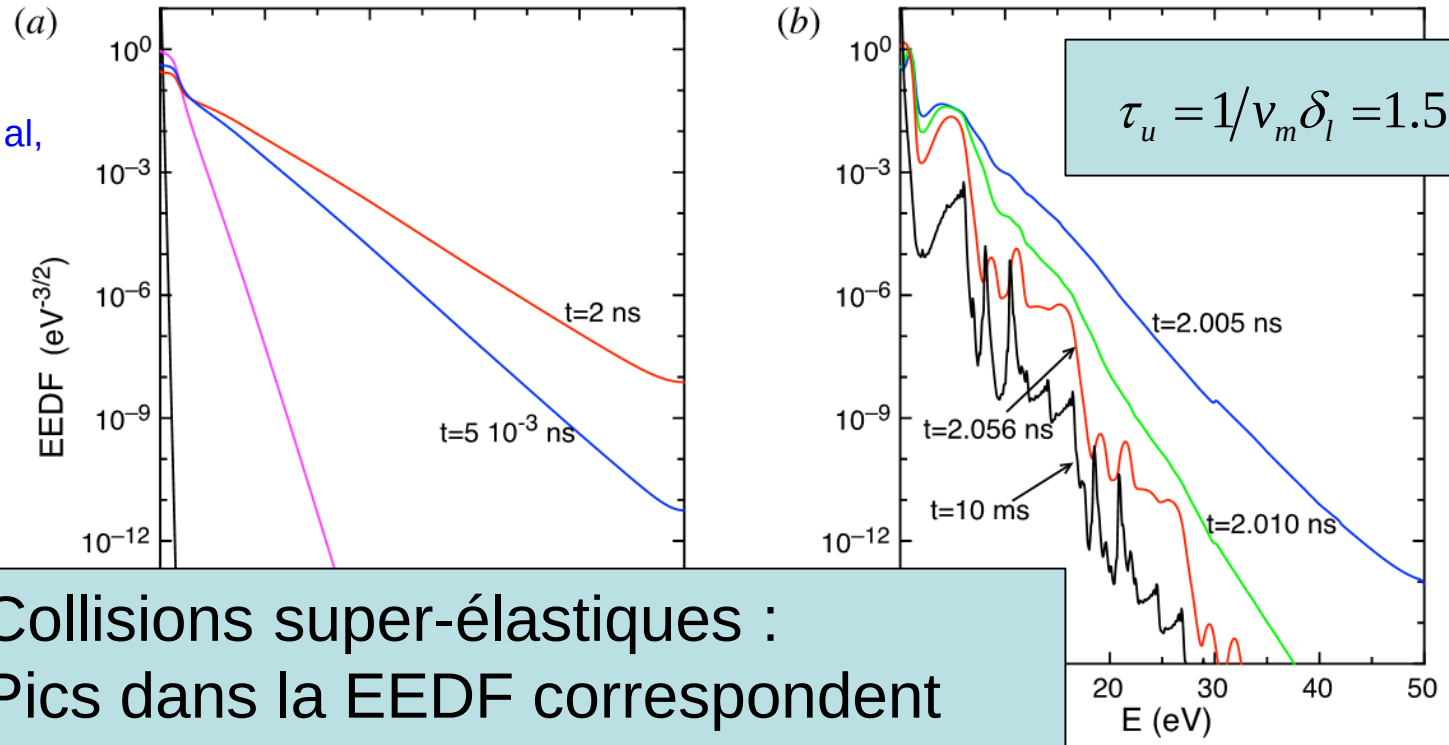

$$\tau_u = 1/\nu_m \delta_l = 1.5\times10^{-11}\ \text{s}$$

Collisions super-élastiques :
Pics dans la EEDF correspondent aux énergies des états excités de CO

ge and (*b*) post-discharge conditions for case study 1 ($T_{gas} = 500$ K, $p = 1$ atm, E/N = 200 Td, $\tau_{pulse} = 2$ ns, $\tau_{afterglow} = 10$ ms).

$\tau_{EEDF} = (n_{CO}K^{1,0}_{eV})^{-1}$	$\tau_{e-V} = (n_e K^{1,0}_{eV})^{-1}$	$\tau_{V-V} = (n_{CO}K^{1,0}_{1,0})^{-1}$	$\tau_{V-T(CO)} = (n_{CO}K^{1,0}_{vT(CO)})^{-1}$	$\tau_{V-T(C,O)} = (n_C K^{1,0}_{vT(C,O)})^{-1}$
4.80×10^{-12} s	3.22×10^{-7} s	4.37×10^{-8} s	5.56×10^{-2} s	3.50×10^{-7} s

TABLE 2. Characteristic times evaluated at the end of the pulse ($\tau_{pulse} = 2$ ns) when the electron density is approximatley 2.2×10^{14} cm^{-3}.

Exemple faiblement ionisé dans le N_2

Colonna et al, PSST 2015

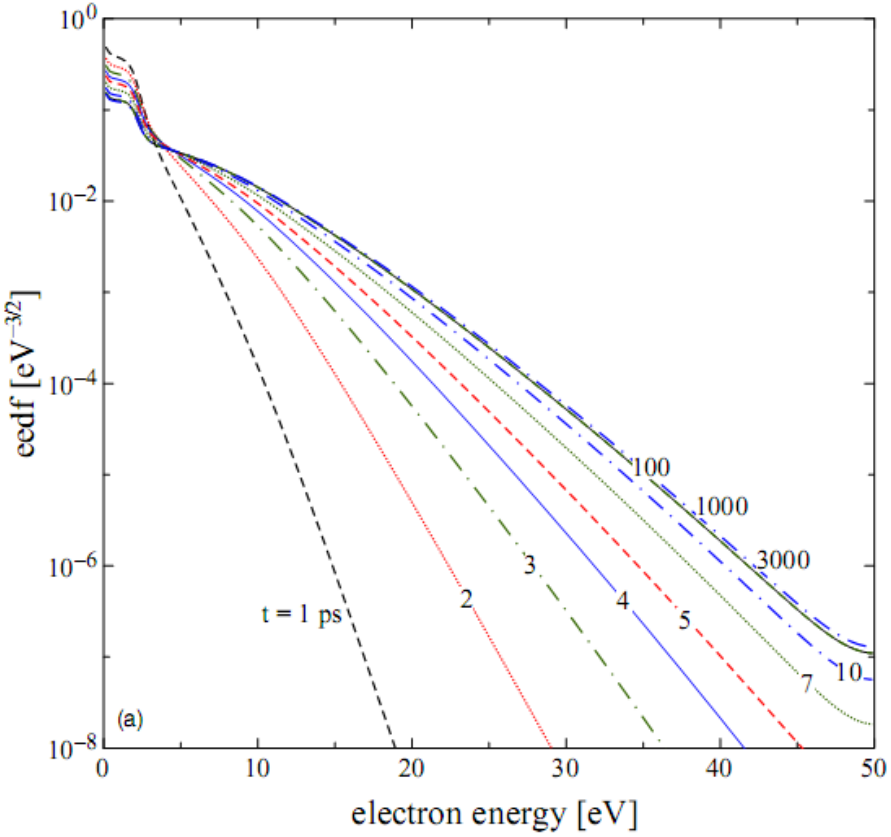

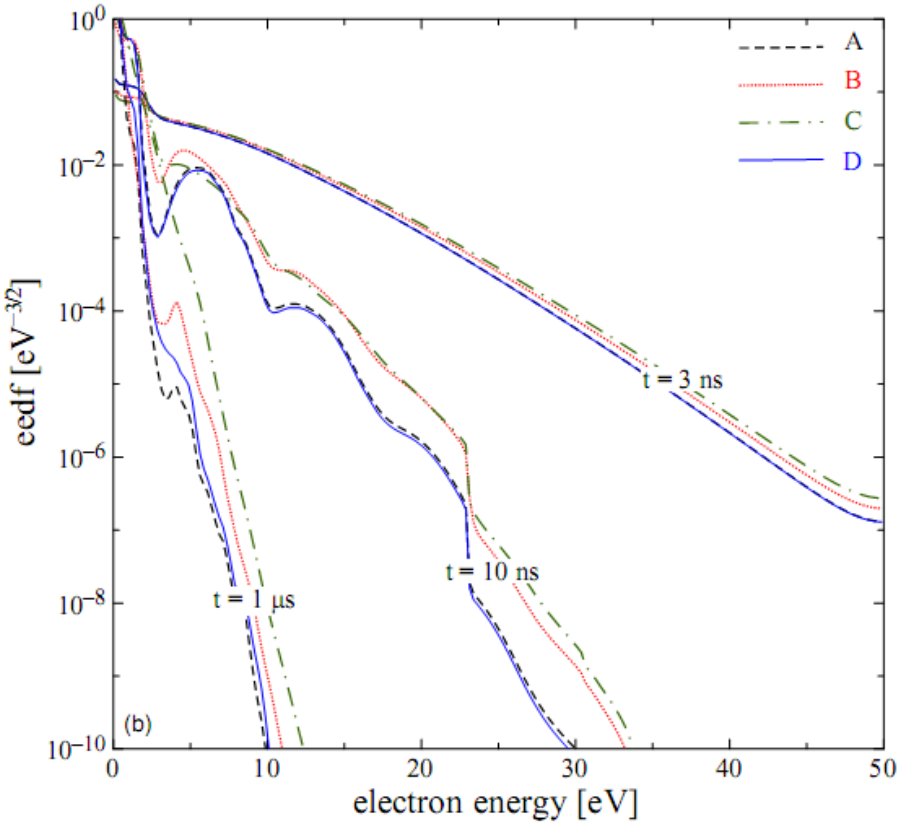

$$e(\epsilon) + N_2(A\ ^3\Sigma) \rightarrow e(\epsilon + \epsilon^*) + N_2(X\ ^1\Sigma_g^+, v)$$

$$e(\epsilon) + N_2(B\ ^3\Pi) \rightarrow e(\epsilon + \epsilon^*) + N_2(X\ ^1\Sigma_g^+, v)$$

$$e(\epsilon) + N_2(C\ ^3\Pi) \rightarrow e(\epsilon + \epsilon^*) + N_2(X\ ^1\Sigma_g^+, v)$$

Exemple fortement ionisé dans l'air

Orrière et al, J Phys D 2018

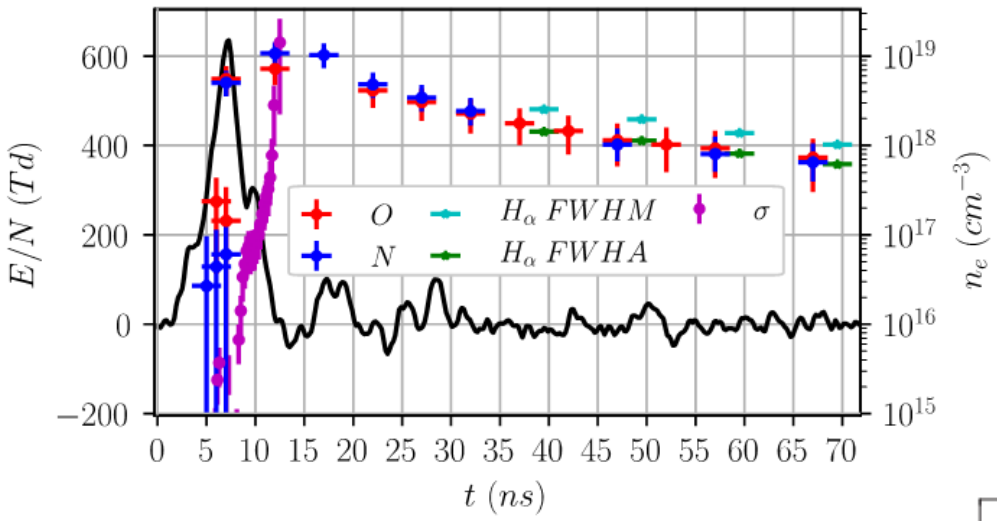

Minesi et al, PSST 2020

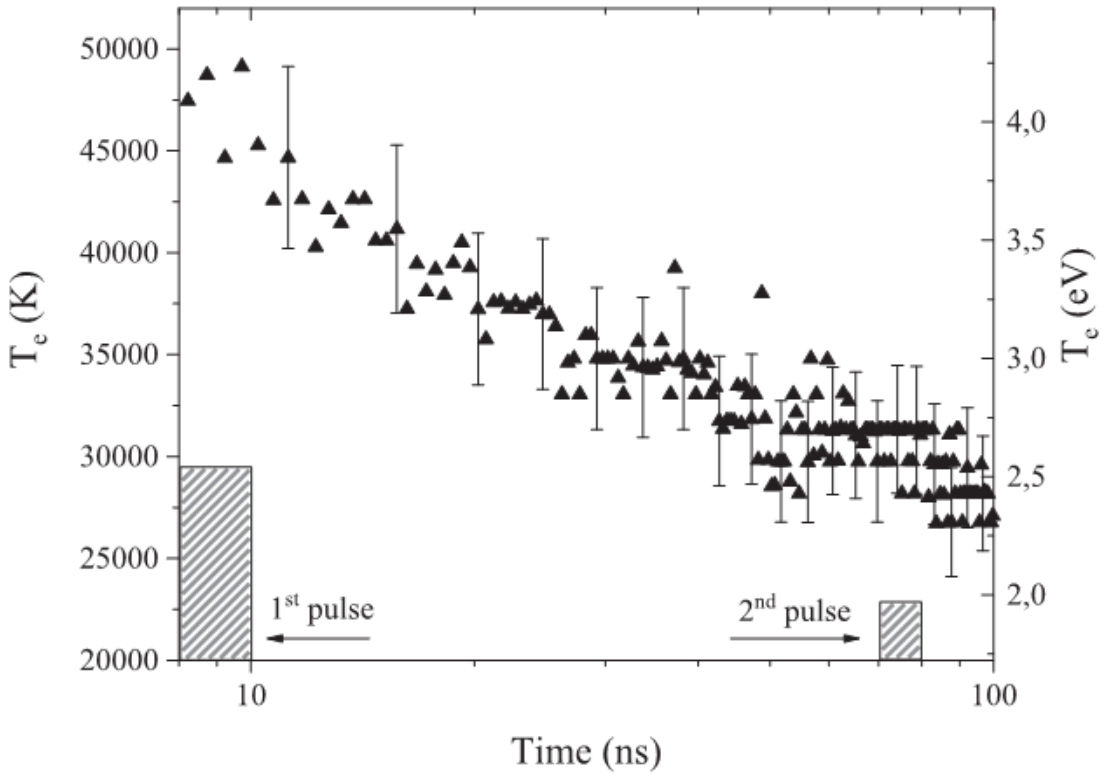

INSTITUT P'

Jo

Exemple fortement ionisé dans l'air

Orrière et al, J Phys D 2018

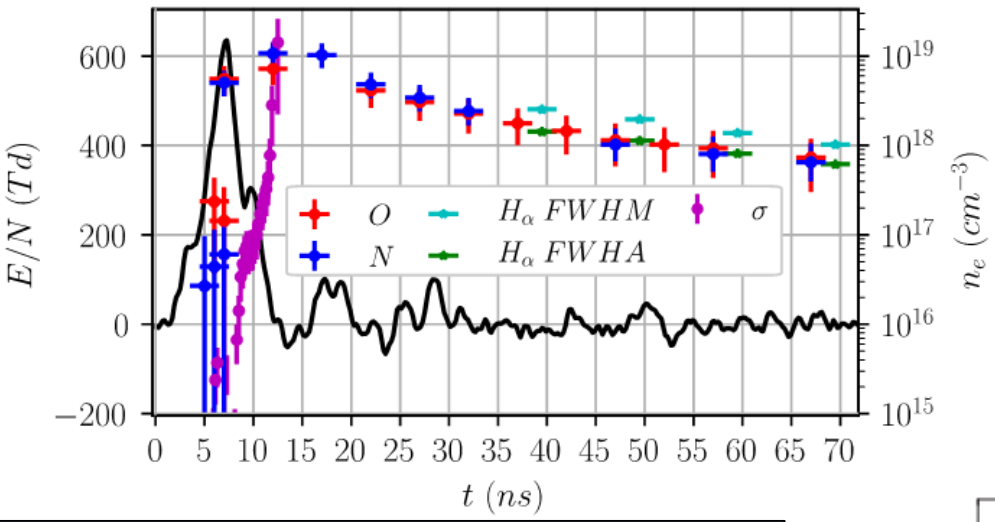

Minesi et al, PSST 2020

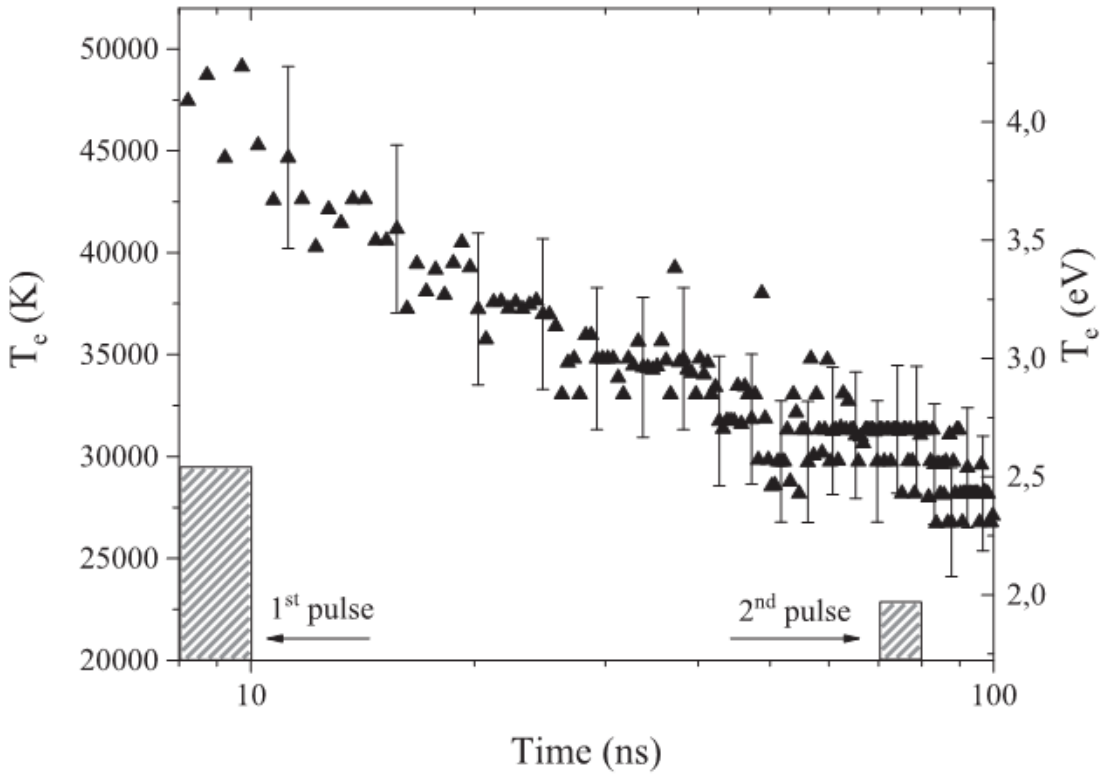

Densité de gaz *N* :

T_g = 350 K initialement

×2 à cause de ~100% ionisation

÷2^3 à cause d'expansion sphérique

$$\nu_m = N\sigma_m\sqrt{8k_BT_e/\pi m_e} = 0.22\ \text{THz}$$

$$\delta_l = 2m_e/m_0 = 7.8\times10^{-5}$$

$$\tau_u = 1/\nu_m\delta_l = 58\ \text{ns}$$

Exemple fortement ionisé dans l'air

Orrière et al, J Phys D 2018

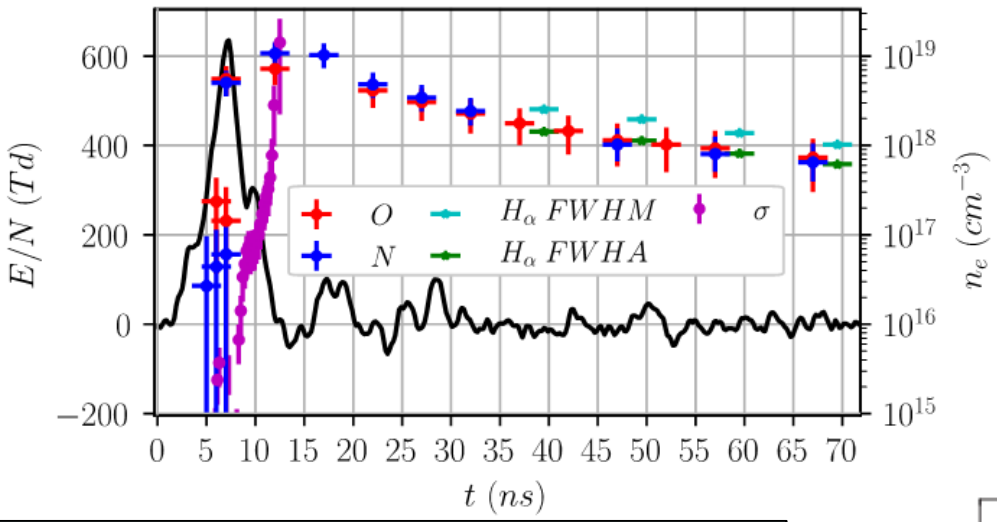

Attention : collisions électrons-ions

$$\nu_m = N \mathrm{v}_d Q_N + n_e \mathrm{v}_d Q_{coul}$$

Densité de gaz *N* :

T_g = 350 K initialement

×2 à cause de ~100% ionisation

÷2^3 à cause d'expansion sphérique

Avec collisions électrons-ions :

$$\nu_m = 0.22 - 2.2 \text{ THz}$$

$$\delta_l = 2m_e/m_0 = 7.8\times10^{-5}$$

$$\tau_u = 1/\nu_m\delta_l = 5.8 - 58 \text{ ns}$$

Minesi et al, PSST 2020

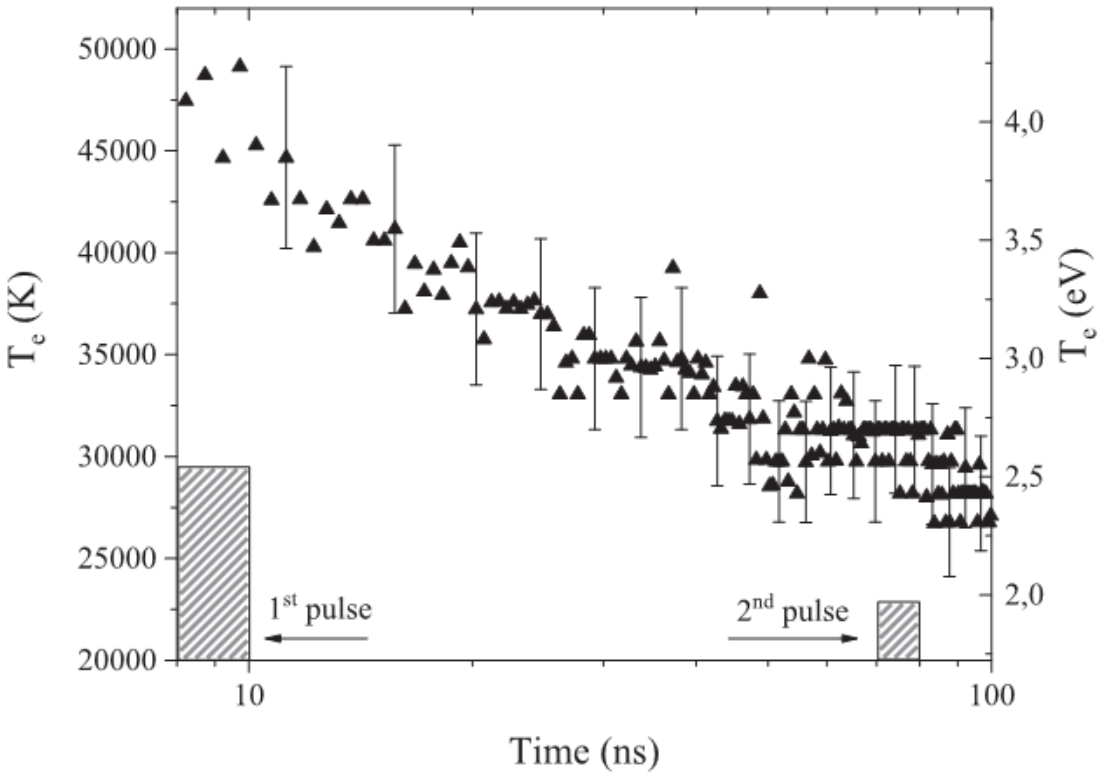

Refroidissement longue des électrons

Miles et al, PSST 2020

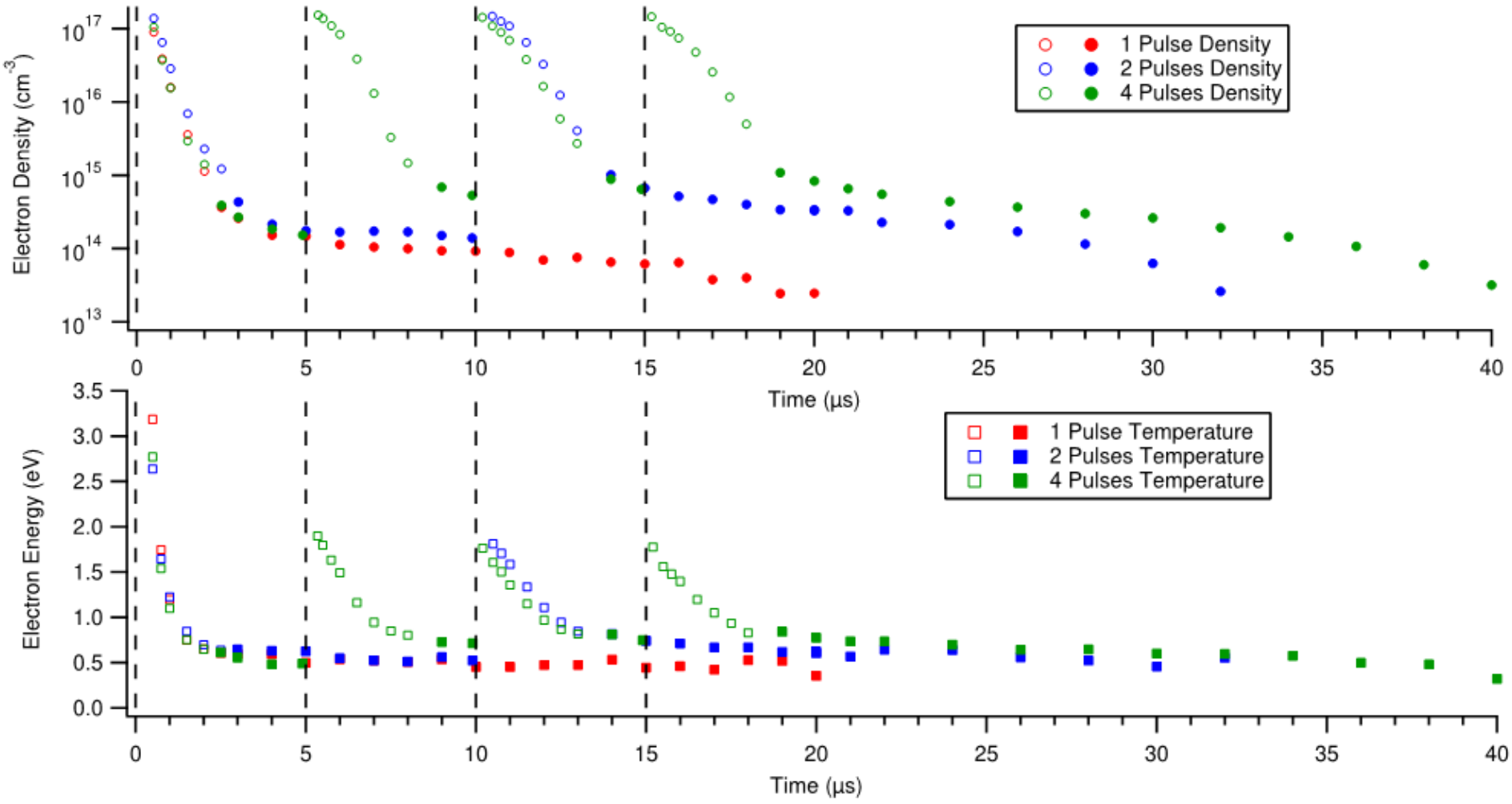

Figure 4. *Top*: Electron densities for three different conditions; 1 pulse, 2 pulses at 100 kHz and 4 pulses at 200 kHz. *Bottom*: electron temperatures for the three conditions. Open and closed symbols indicate whether electron parameters were measured with collective or non-collective Thomson scattering, respectively. The black dashed vertical lines indicate when an additional electrical pulse was applied in the 2 and 4 pulse data sets. Uncertainties for collective data points are approximately 5%, while non-collective data points are 10%.

Gaz moléculaire dissocié versus gaz atomique

Minesi et al, PSST 2020

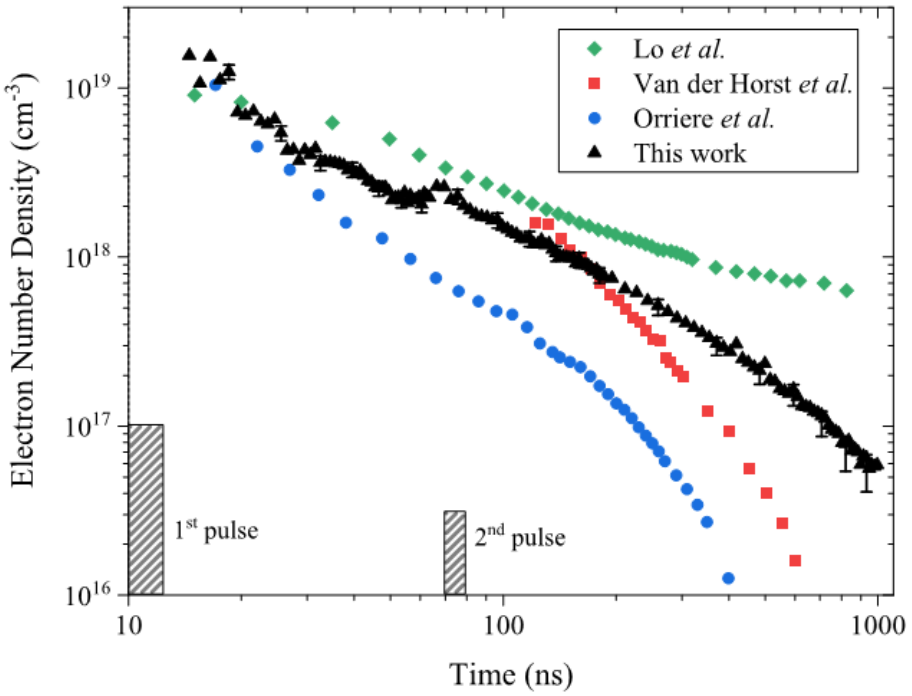

Figure 13. Decay of the electron number density, measured from the Stark broadening of H_α (black triangles). The increase of n_e at $t \approx 70$ ns is caused by the reflected pulse. The measurements performed by van der Horst *et al* in $N_2 + 0.9\%$ H_2O [12] (red squares), Orrière *et al* in air [13] (blue circles), and Lo *et al* in air [9] (green diamonds) are shown for comparison.

Zhu et al, J Phys D 2012

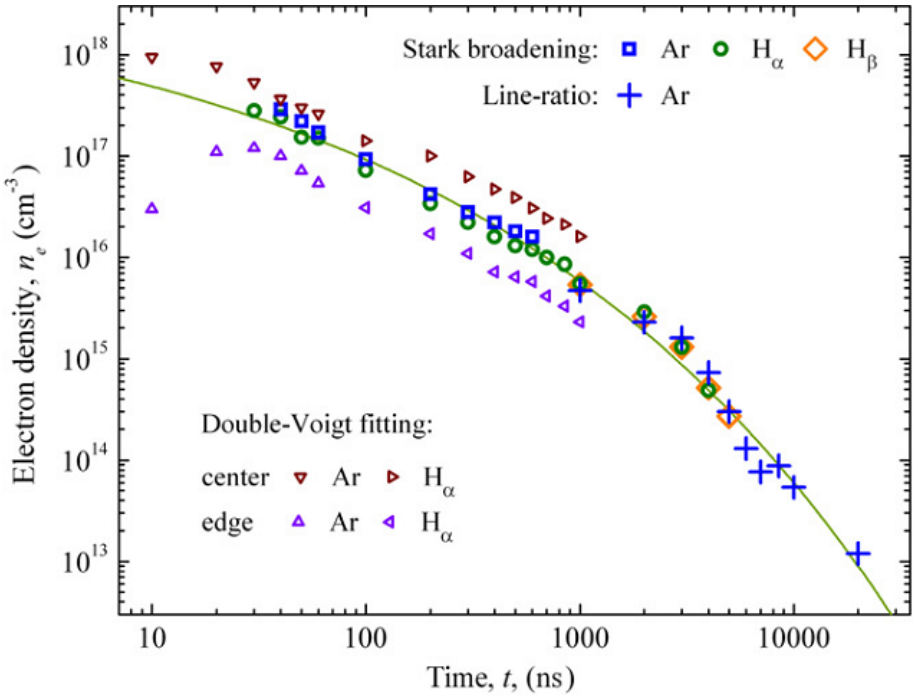

Figure 11. Experimentally measured electron densities in a high-pressure nanosecond pulsed microplasma (Ar/Ne = 700/30 Torr, discharge current lasts for about 100 ns, pulse period 1 ms). In the legend on the right top, 'line ratio' refers to the line-ratio method and 'Stark broadening' refers to the Stark broadening method using Ar 696.5 nm, H_α and H_β lines with a single-Voigt fitting procedure. In the legend on the left bottom, 'centre' and 'edge' denote $n_{e,centre}$ and $n_{e,edge}$ obtained with double-Voigt fitting. The solid line shows a function, $n_e = 6 \times 10^{18} \times \exp(-(t/0.15)^{0.22})$, where n_e and t are in units of cm^{-3} and ns, respectively.

Champ électrique

1) Choisir E/N, τ_{pulse}
2) Connaître N
3) Appliquer E = V/d pendant τ_{pulse}

Champ électrique

1) Choisir E/N, τ_{pulse}
2) Connaître N
3) Appliquer E = V/d pendant τ_{pulse}
4) Ecrantage du champ électrique

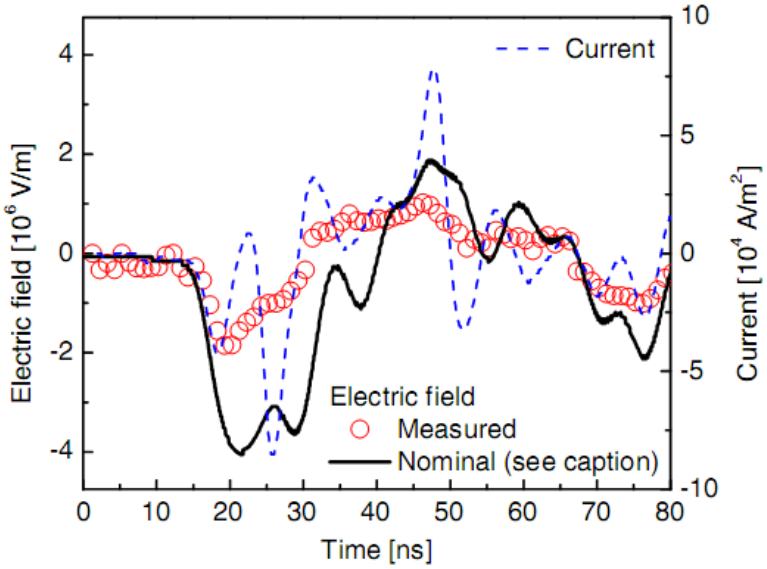

FIG. 1 (color online). Temporal evolution of the nominal electric field (the electric field expected without any space charge: solid curve), electric field at the center of the gap measured by E-CRS (empty circle), and the current (dashed curve).

Ito et al, Phys Rev Lett 2011

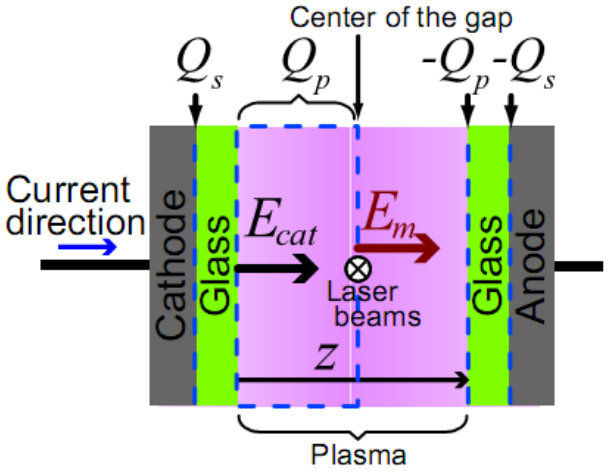

FIG. 2 (color online). A schematic diagram of the discharge system. The arrows illustrate the sign convention of current and electric-field directions employed in this study. The electric field was measured by E-CRS at the center of the electrode gap, and its value is denoted by E_m. The electric field at the cathode is denoted by E_{cat}.

Table 9.1. Time scales of various discharge processes under conditions typical of discharge in cw CO_2 lasers ($CO_2 + N_2 + He$); $p \sim 10$–100 Torr, $N \sim 10^{18}\,10^{-3}$, $T \sim 300$–500 K, $E/p \sim 10$ V/(cm·Torr), $T_e \approx 1$ eV, $T_V \approx 2000$–5000 K, $n_e \sim 10^{10}$ cm^{-3}, $\Lambda \sim 1$ cm [a)]

Process	Characteristic time	Duration, s
1. Space-charge relaxation	$\tau_\sigma = 1/4\pi\sigma$	10^{-10}–10^{-9}
2. Collisional energy transfer		
(1) electron tempeature relaxation	$\tau_u = 1/\nu_m\delta_1$	10^{-9}–10^{-8}
(2) gas heating	$\tau_T = Nc_{p1}T/\sigma E^2$	10^{-3}–10^{-2}
(3) pumping of molecular vibrations	$\tau_V = N_M c_V T_V/\sigma E^2$	10^{-3}–10^{-2}
(4) vibrational relaxation	τ_{VT}	10^{-4}–10^{-2}
3. Collision kinetics		
(1) ionization	$\tau_i = (k_i N)^{-1}$	10^{-5}–10^{-4}
(2) attachment	$\tau_a = (k_a N)^{-1}$	10^{-6}–10^{-5}
(3) detachment	$\tau_d = (k_d N)^{-1}$	10^{-6}–10^{-5}
(4) electron excitation	$\tau^* = (k^* N)^{-1}$	10^{-6}–10^{-4}
(5) electron-ion recombination	$\tau_{rec}^e = (\beta_e n_+)^{-1}$	10^{-4}–10^{-3}
(6) ion-ion recombination	$\tau_{rec}^- = (\beta_- n_+)^{-1}$	10^{-4}–10^{-3}
4. Transport processes		
(1) pressure levelling (sound)	$\tau_s = \Lambda/c_s$	10^{-5}–10^{-4}
(2) heat conduction of the gas	$\tau_\chi = \Lambda^2/\chi$	10^{-2}
(3) ambipolar diffusion	$\tau_{da} = \Lambda^2/D_a$	10^{-2}
(4) electron heat conduction	$\tau_\chi^e = \Lambda^2/\chi_e$	10^{-5}

Temps de Maxwell

En unités SI :

$$\tau_\sigma = \varepsilon_0/\sigma$$

Champ électrique

1) Choisir E/N, τ_{pulse}
2) Connaître N
3) Appliquer E = V/d pendant τ_{pulse}
4) Ecrantage du champ électrique

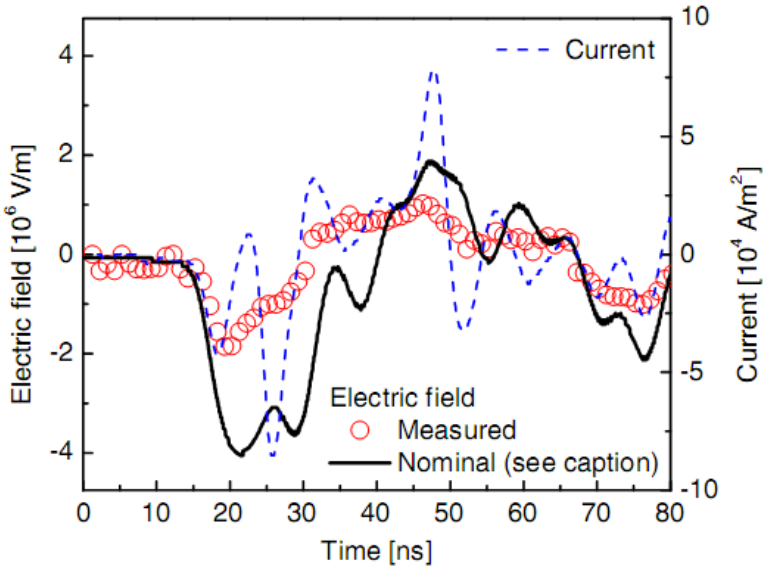

FIG. 1 (color online). Temporal evolution of the nominal electric field (the electric field expected without any space charge: solid curve), electric field at the center of the gap measured by E-CRS (empty circle), and the current (dashed curve).

$$n_e \approx 10^{12}\ \mathrm{cm}^{-3}$$

$$\nu_m \approx 3\ \mathrm{THz}$$

$$\sigma = e^2 n_e / m_e \nu_m \approx 0.01\ \Omega^{-1}\mathrm{m}^{-1}$$

$$\tau_\sigma = \varepsilon_0 / \sigma \approx 1\ \mathrm{ns}$$

Déjà une première idée de l'échelle du temps, à détailler après…

Electrons « runaway »

Gurevich & Zybin, Physics Uspekhi 2001

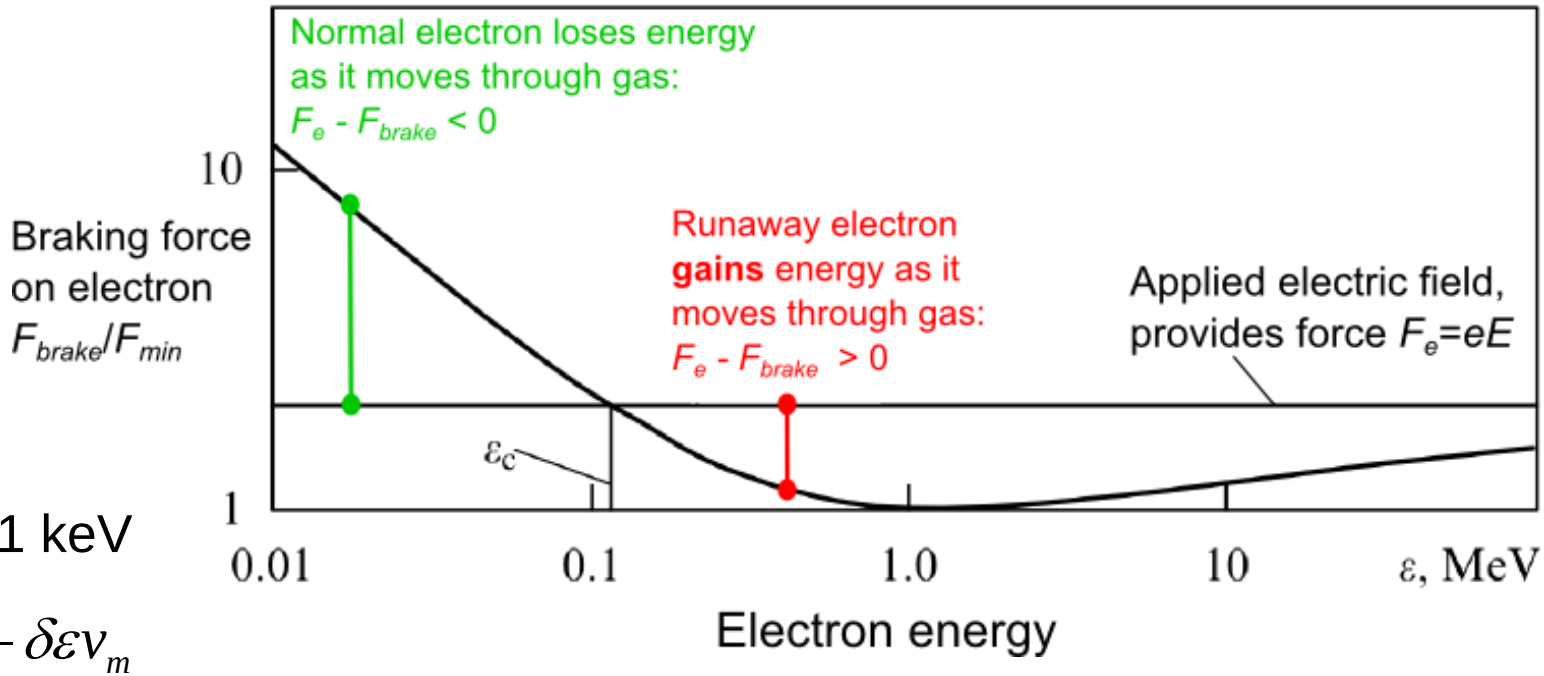

- électrons $\varepsilon < 1$ keV

$$\frac{d\varepsilon}{dt} = eE\mathrm{v}_d - \delta\varepsilon\nu_m$$

- électrons $\varepsilon >> 1$ keV → collisions de Coulomb (électron-ion)

$$\frac{1}{\mathrm{v}_d}\frac{d\varepsilon}{dt} = eE - F_{brake}$$

$$Q_{coul} \propto 1/\varepsilon^2$$

$$F_{brake} \propto \varepsilon Q_{coul} N \propto 1/\varepsilon$$

Lieberman & Lichtenberg p. 56
Mitchner & Kruger p. 58

Electrons « runaway »

Starikovskaia et al, PSST 2001

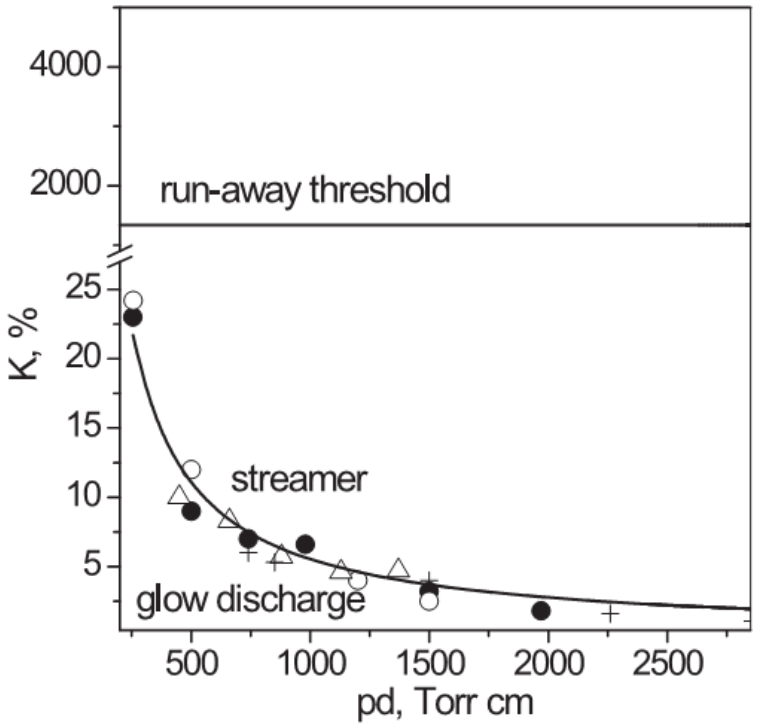

Figure 1. Regions of breakdown development for various mechanisms depending upon the overvoltage in air. The curve which separates the glow discharge and the streamer is taken from [2]. In various points designate different experimental data. The horizontal line represents the runaway threshold for a uniform stationary electric field.

Shao et al, Lasers & Particle Beams 2012

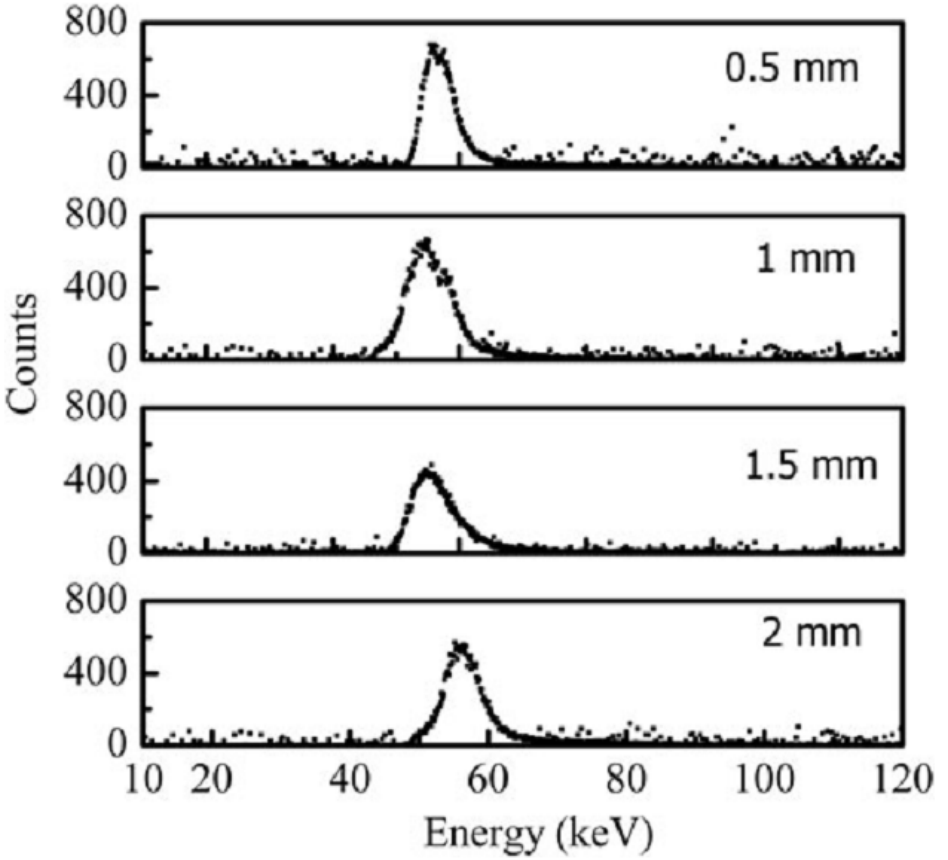

Fig. 7. Energy distribution of X-ray radiation with the cathodes of different curvature radiuses (0.5 mm, 1 mm, 1.5 mm, and 2 mm). Pulser #1. Gap spacing: 8 cm.

DYNAMIQUE DES DECHARGES: TRAITEMENT 1D À 3D

Transition avalanche-streamer

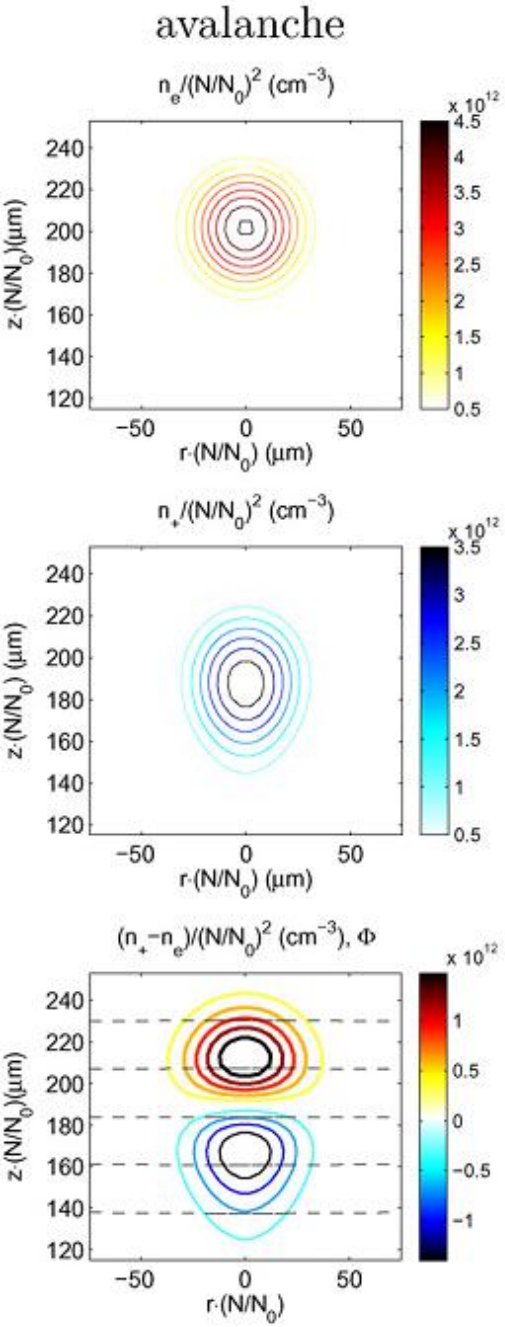

Au départ, l'expansion du nuage des électrons est pilotée par la diffusion:

$$R = \sqrt{2Dt}$$

$$dR/dt = \sqrt{D/2t} \propto t^{-1/2}$$

Mais la diffusion est dépassée par la répulsion une fois la densité de charge devient important:

$$\frac{dR}{dt} = \mu_e E' \propto \exp\left(\nu_{i0} t\right)$$

Parce que :

$$E' = \frac{1}{4\pi\varepsilon_0}\frac{eN_e}{R^2}$$

$$N_e = n_{e0}\exp\left(\nu_{i0} t\right)$$

Transition avalanche-streamer

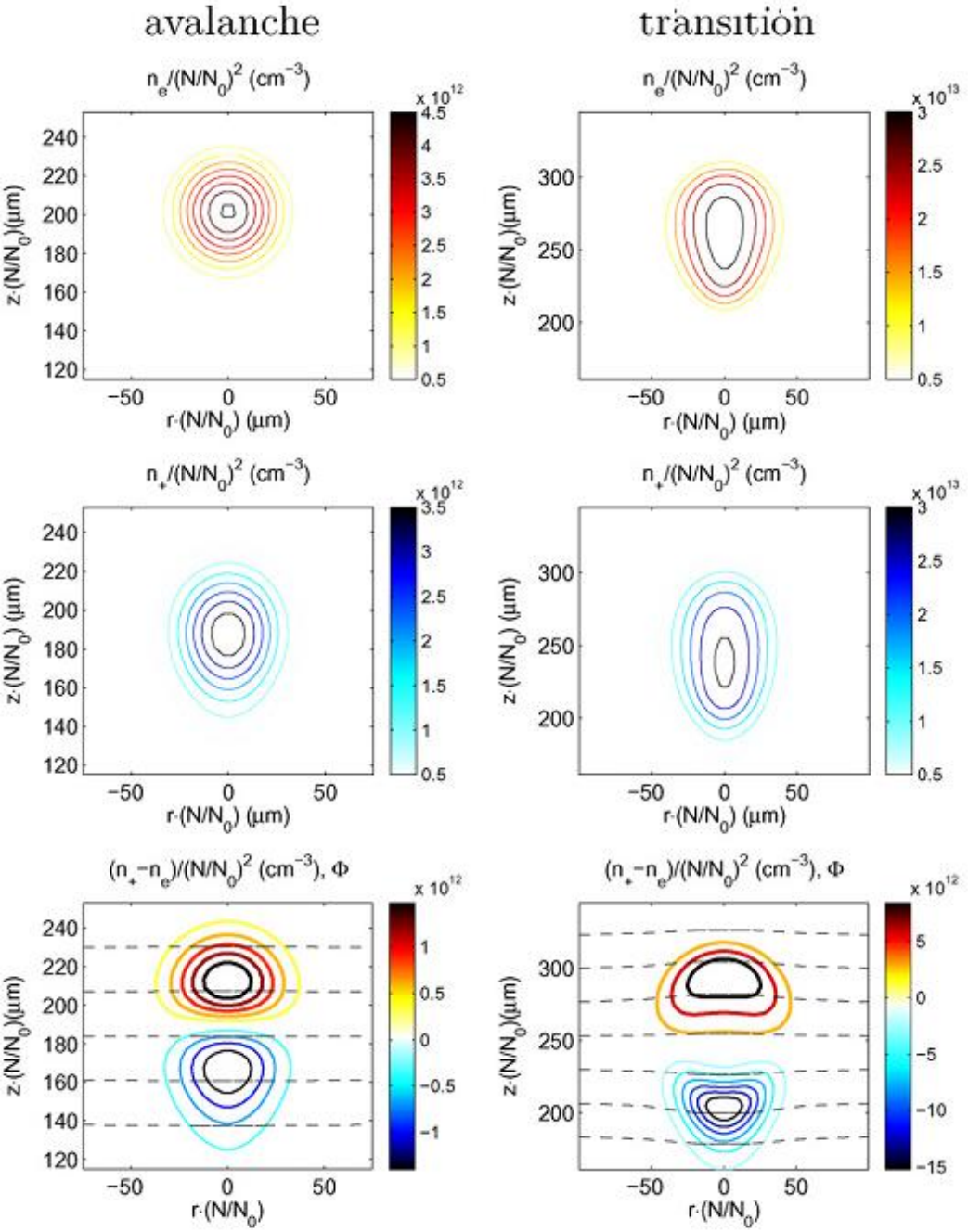

Le temps caractéristique de l'expansion du nuage est déterminé par le temps de Maxwell

$$E' = \frac{1}{4\pi\varepsilon_0}\frac{eN_e}{R^2}$$

$$\frac{dR}{dt} = \mu_e E' = \frac{R}{3\varepsilon_0}\underbrace{\left(\underbrace{\frac{3N_e}{4\pi R^3}}_{n_e}\cdot e\mu_e\right)}_{\sigma}$$

$$\frac{dR}{dt} = \frac{1}{3}\frac{R}{\tau_\sigma}$$

Transition avalanche-streamer

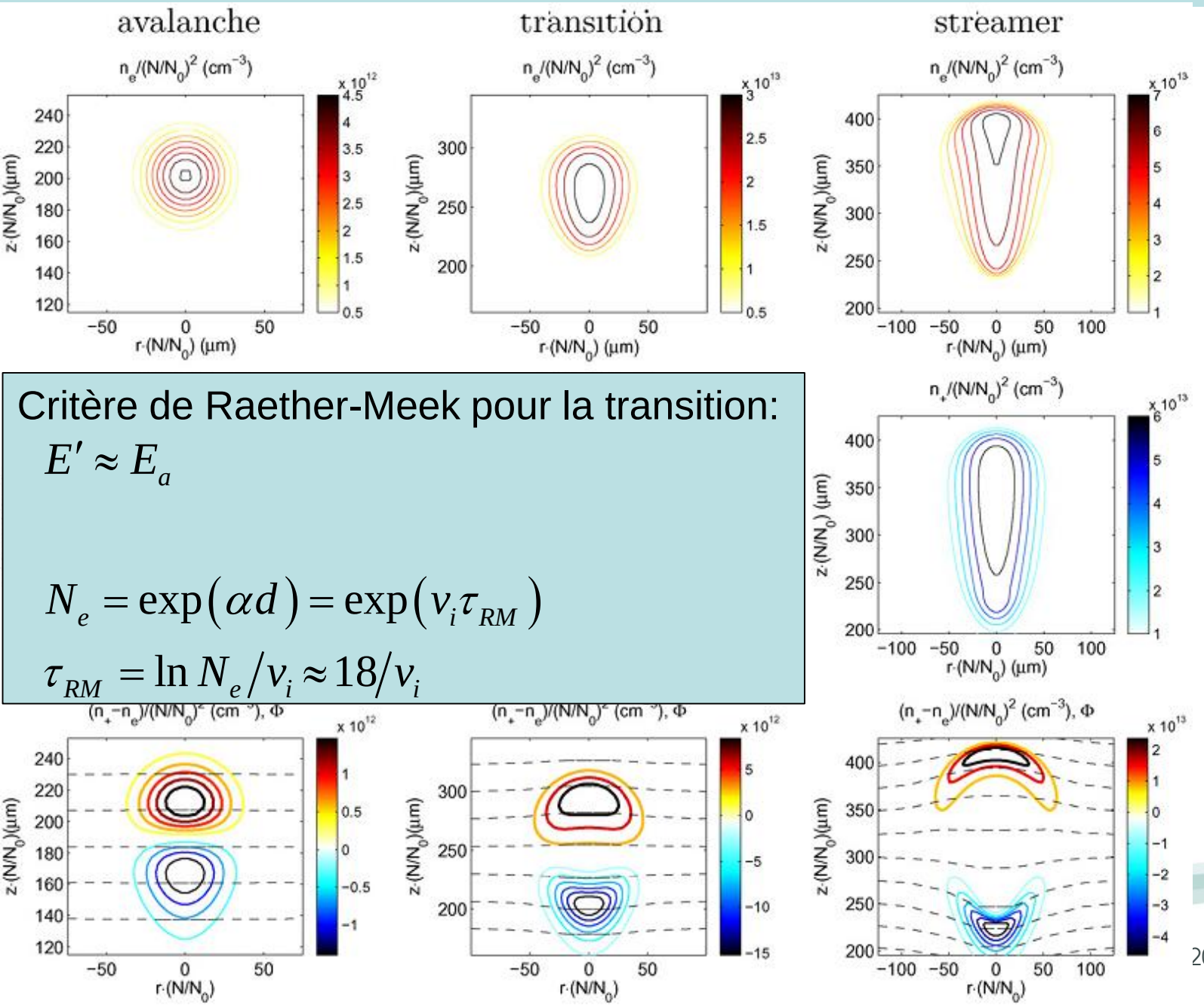

Critère de Raether-Meek pour la transition:

$$E' \approx E_a$$

$$N_e = \exp(\alpha d) = \exp(v_i \tau_{RM})$$

$$\tau_{RM} = \ln N_e / v_i \approx 18/v_i$$

Montijn & Ebert, J Phys D 2006

Propagation du streamer

Sébastien Célestin, PhD Thesis, Ecole Centrale Paris, 2008

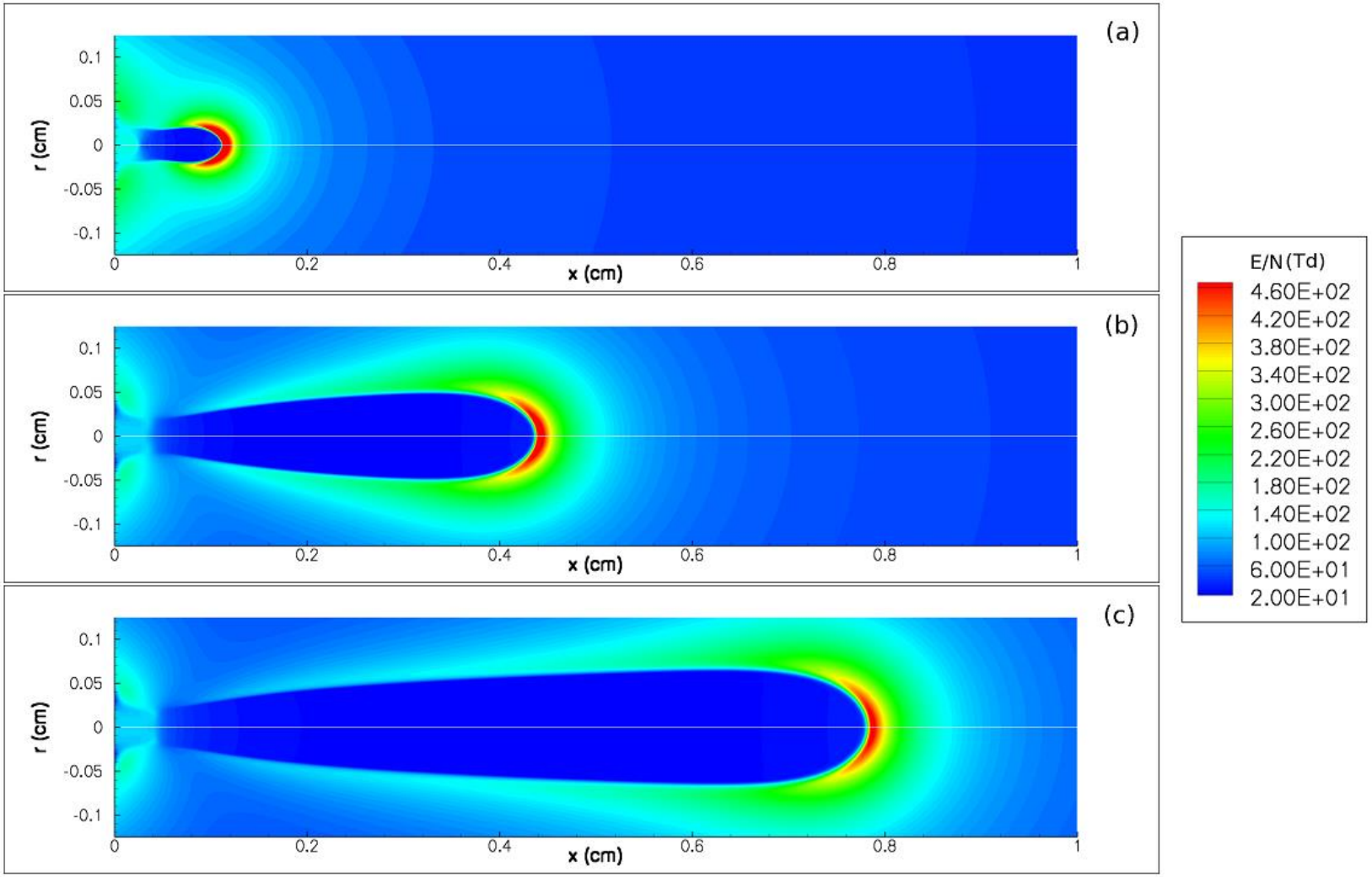

Figure II.8: Cross-sectional view of the distribution of the electric field at different times, computed using the upwind scheme. (a) $t = 2.5$ ns. (b) $t = 8.5$ ns. (c) $t = 14.5$ ns. (1 Td=10^{-17} V cm^2).

Propagation du streamer

Sébastien Célestin, PhD Thesis, Ecole Centrale Paris, 2008

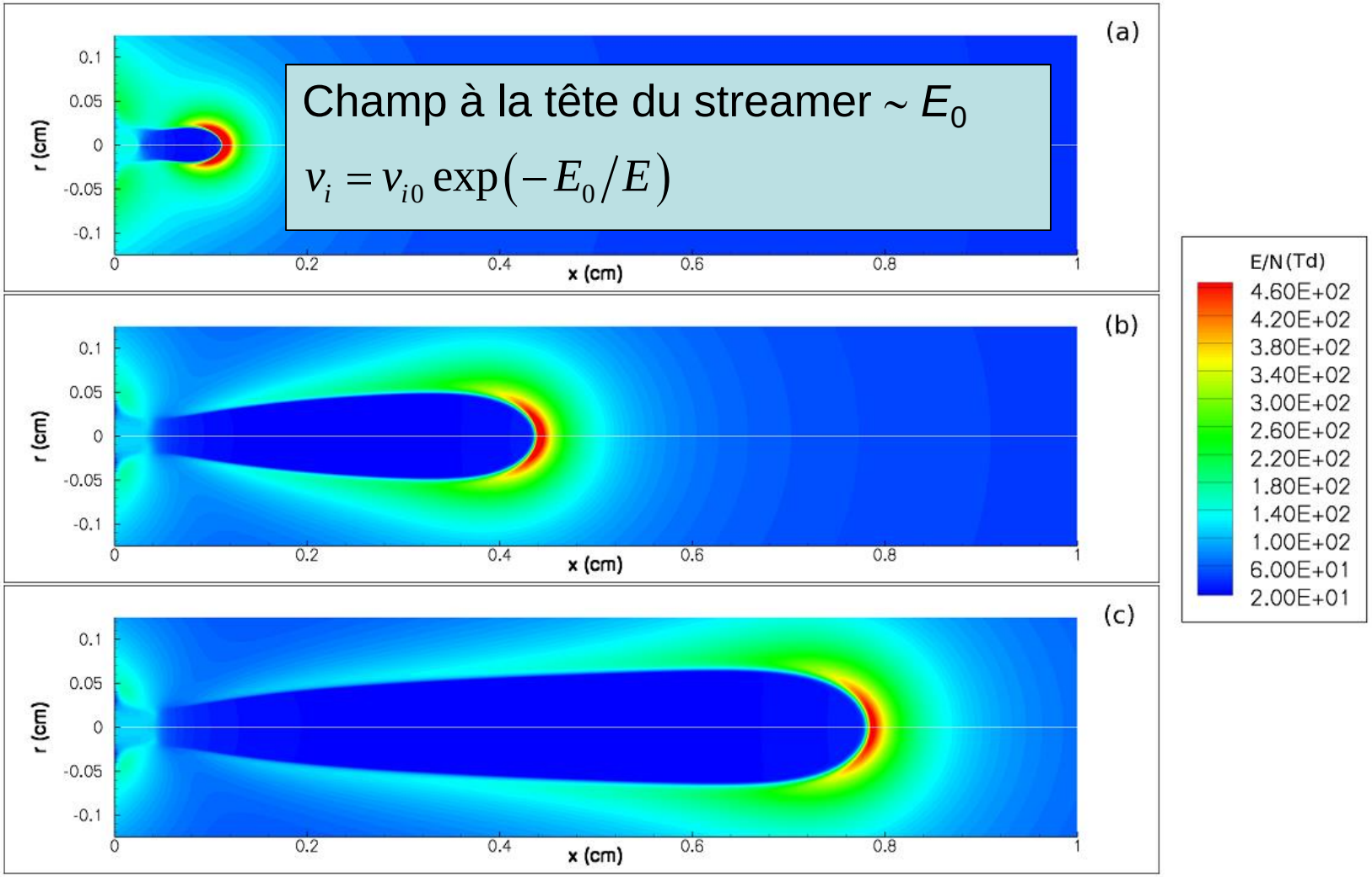

Figure II.8: Cross-sectional view of the distribution of the electric field at different times, computed using the upwind scheme. (a) $t = 2.5$ ns. (b) $t = 8.5$ ns. (c) $t = 14.5$ ns. (1 Td=10^{-17} V cm^2).

Propagation du streamer

D'yakonov & Kachorovskii, Zh. Eksp. Teor. Fiz. (Soviet JETP), 1988

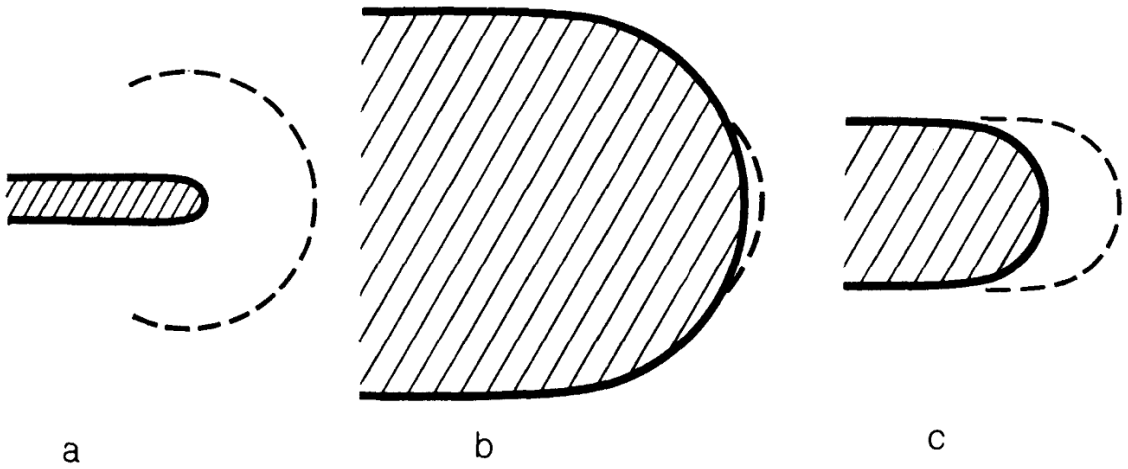

FIG. 1. Diagram explaining the relation $E_m \sim E_0$. The shaded region is the streamer head. The impact-ionization region is bounded by the dashed line: a—$E_m \gg E_0$, b—$E_m \ll E_0$, c—$E_m \sim E_0$.

$$\nu_i = \nu_{i0} \exp\left(-E_0/E\right)$$

Propagation du streamer

Sébastien Célestin, PhD Thesis, Ecole Centrale Paris, 2008

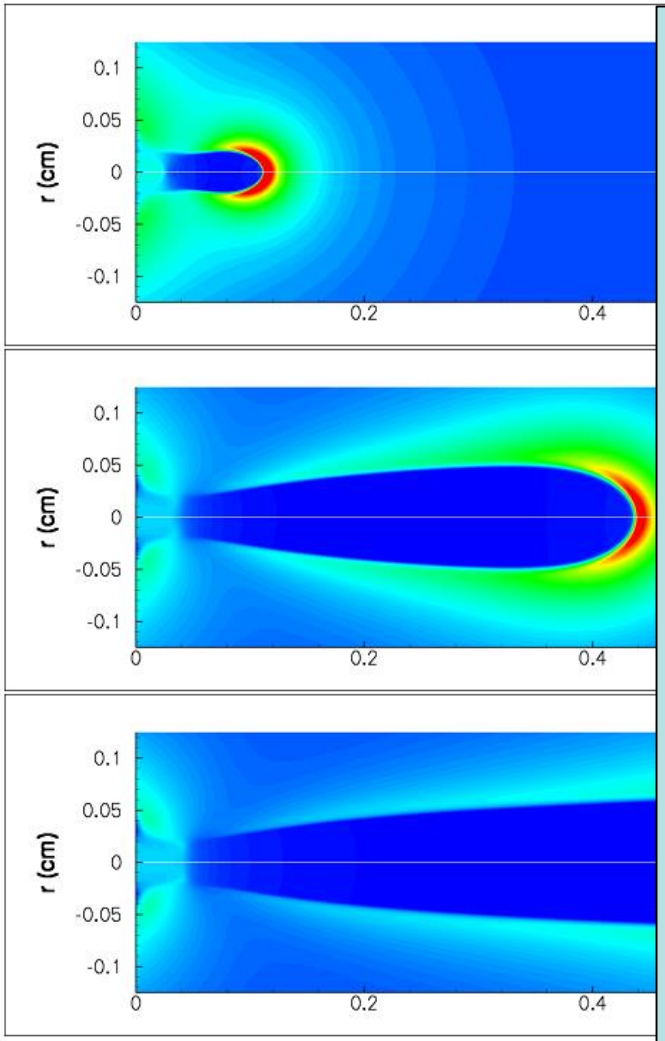

Figure II.8: Cross-sectional view of
computed using the upwind scheme. (a) t = 2.5 ns. (b) t = 8.5 ns. (c) t = 14.5 ns. (1
Td=10^{-17} V cm^2).

D'yakonov & Kachorovskii, Zh. Eksp. Teor. Fiz. (Soviet JETP), 1988
Bazelyan & Raizer, "Spark Discharge", 1998
Kulikovsky, Phys Rev E, 1998

Ionisation peut progresser tant que le champ n'est pas écranté :

$$1/\tau_\sigma = \varepsilon_0/\sigma \approx \nu_{i0}$$

Le temps nécessaire pour l'écrantage :

$$e\mu_e n_{e0} \exp(\nu_{i0}\tau) \approx \varepsilon_0 \nu_{i0}$$

$$\tau \approx \frac{\ln(\varepsilon_0 \nu_{i0}/e\mu_e n_{e0})}{\nu_{i0}} = \frac{\ln(n_e/n_{e0})}{\nu_{i0}}$$

L'écrantage a lieu dans la tête du streamer :

$$v_s \approx \frac{R}{\tau} = \frac{\nu_{i0} R}{\ln(N/n_{e0})}$$

Préionisation

Palmer, APL 1974
Levatter et Lin, JAP 1980

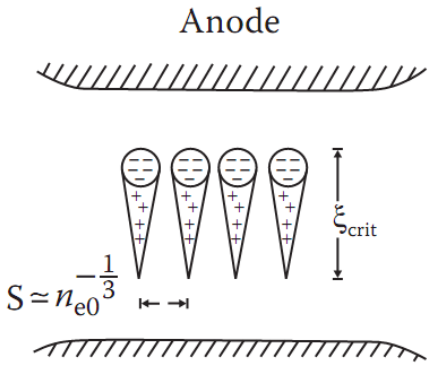

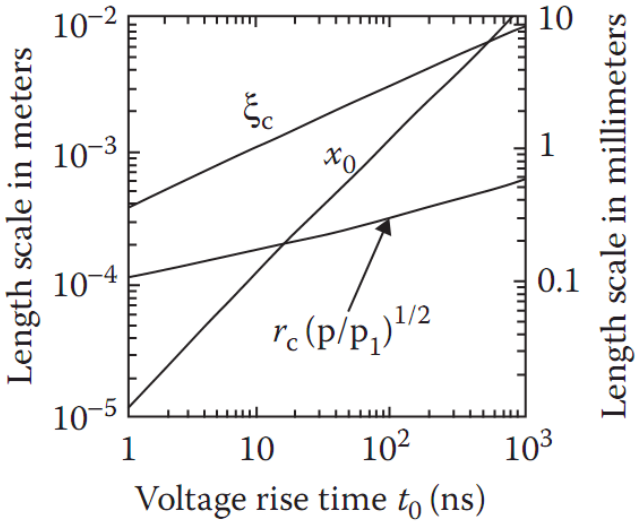

Lorsque les nuages sont toujours diffusifs :

$$t = \xi_{crit} / v_d$$

$$R_{crit} = \sqrt{2Dt} = \sqrt{\frac{2D\xi_{crit}}{\mu_e E}}$$

Empêchement de la transition avalanche-streamer par chevauchement des nuages :

$$\alpha \xi_{crit} \approx 18 \qquad \text{(critère Raether-Meek)}$$

$$n_{e0} > 1/R_{crit}^3$$

Dans l'air à 1 atm:
α = 1000 cm^{-1}, D/μ_e = 15 V, E = 100 kV/cm $\rightarrow$
ξ_{crit} = 160 µm, R_{crit} = 24 µm, $n_{e0} > 10^8$ cm^{-3}

Préionisation

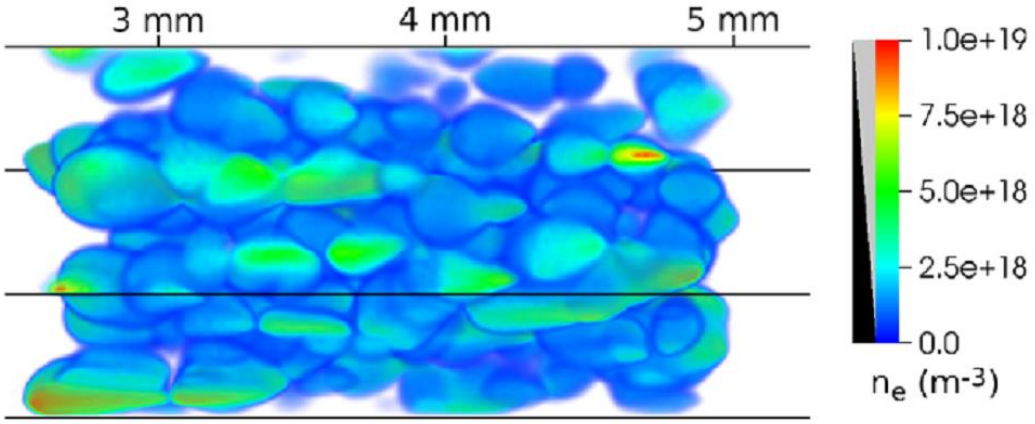

Teunissen et al, J Phys D, 2014

Figure 7. The electron density in the 3D particle model at 5.25 ns, for an initial density of $n_0 = 10^{11}$ m^{-3}.

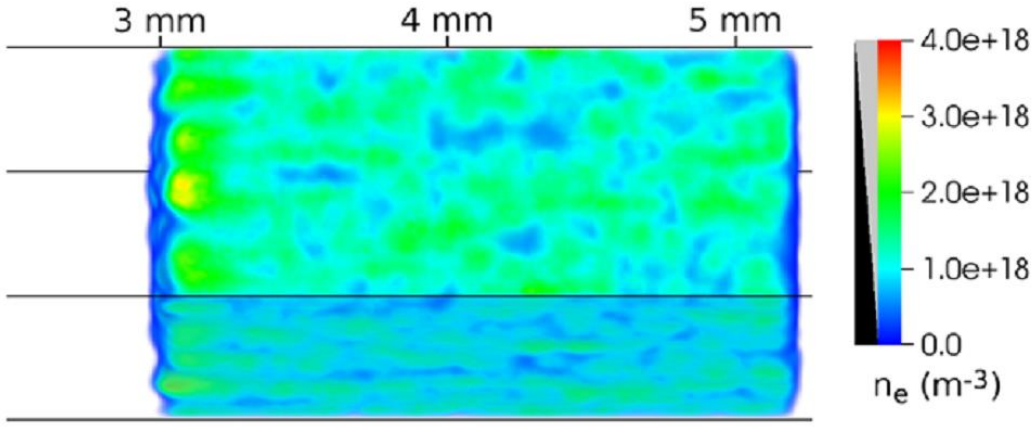

Figure 5. The electron density in the 3D particle model at 4.05 ns, for an initial density of $n_0 = 10^{13}$ m^{-3}. (This figure is made using volume rendering; transparency is indicated in the legend.)

Préionisation

Tholin et Bourdon, J Phys D 2011

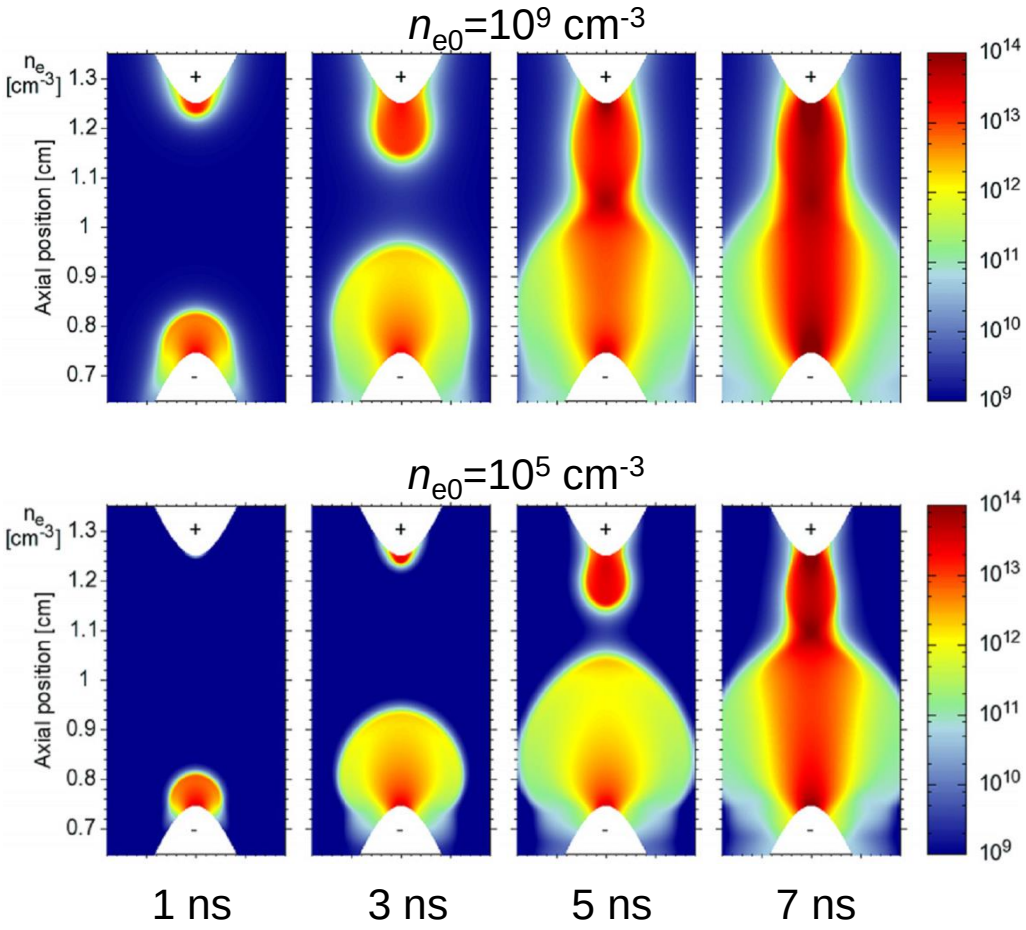

À T_g=300 K dans l'air à 1 atm :

- la préionisation est portée par les ions négatifs/positifs
- photo-ionisation n'est plus nécessaire pour la propagation des streamers

Changement de la vitesse de propagation des streamers

Région cathodique

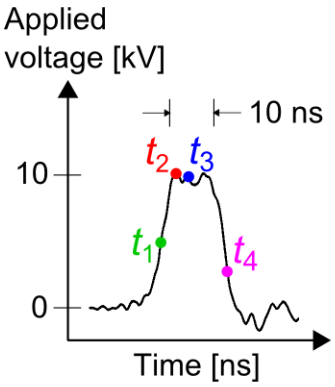

E_L = Laplacian field
E_{SC} = space-charge field
$E = E_L + E_{SC}$

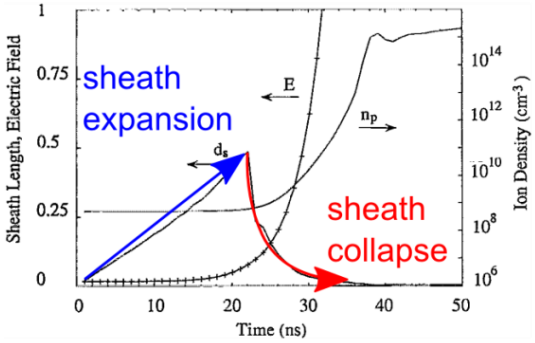

Belasri et al, JAP 1993

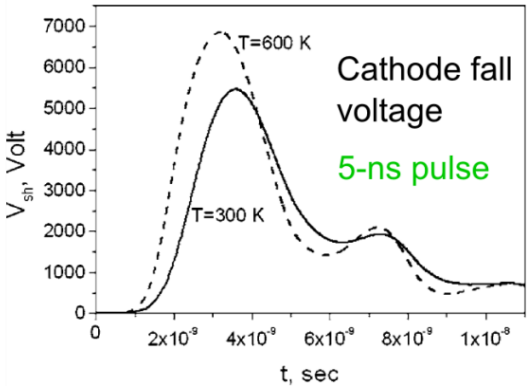

Macheret et al,
Phys Plasmas 2006

Net charge in discharge gap

t_1
Avalanche

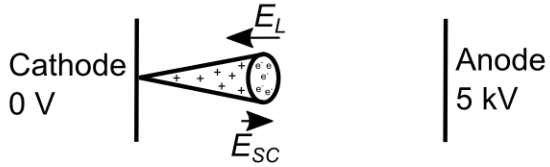

t_2
Cathode sheath expansion

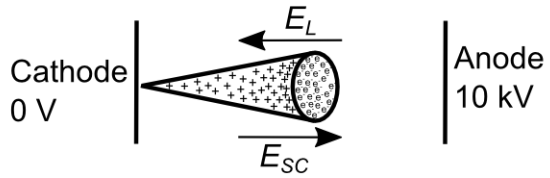

- Electrons "swept out", leaving ion layer
- Continues until $E_L = E_{SC}$

t_3
Cathode sheath collapse

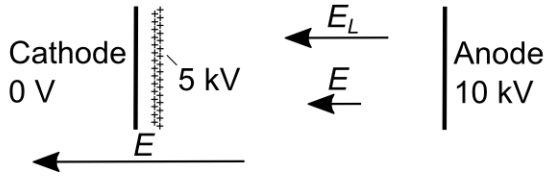

- Streamer-like ionization front moves plasma-sheath boundary

REGIMES DES DECHARGES

Nanosecond Repetitively Pulsed (NRP) discharges

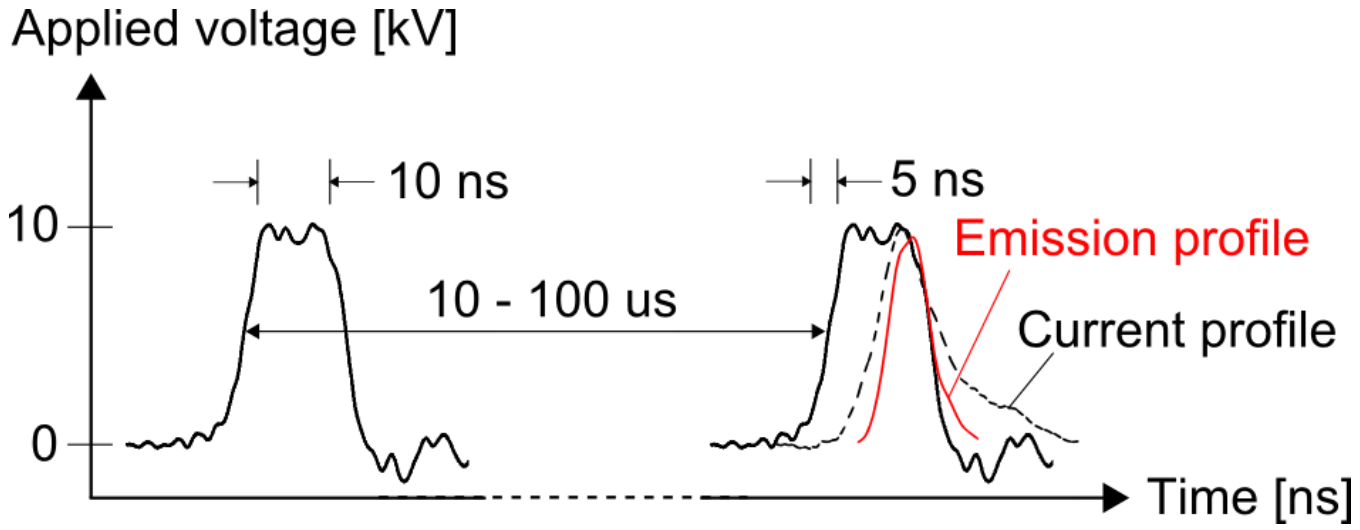

- Utiliser une Pulse Repetition Frequency (PRF) élevée
  - 1/PRF < temps de recombinaison du plasma (électrons, espèces radicaux, métastables)
  - Accumulation des espèces
  - Augmentation du niveau de préionisation

Régimes des décharges NRP

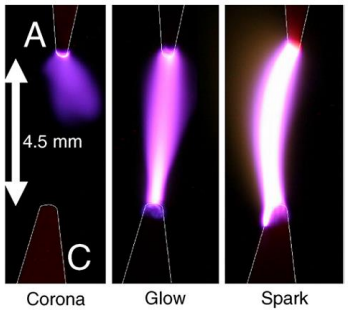

Pai et al, JAP 2010

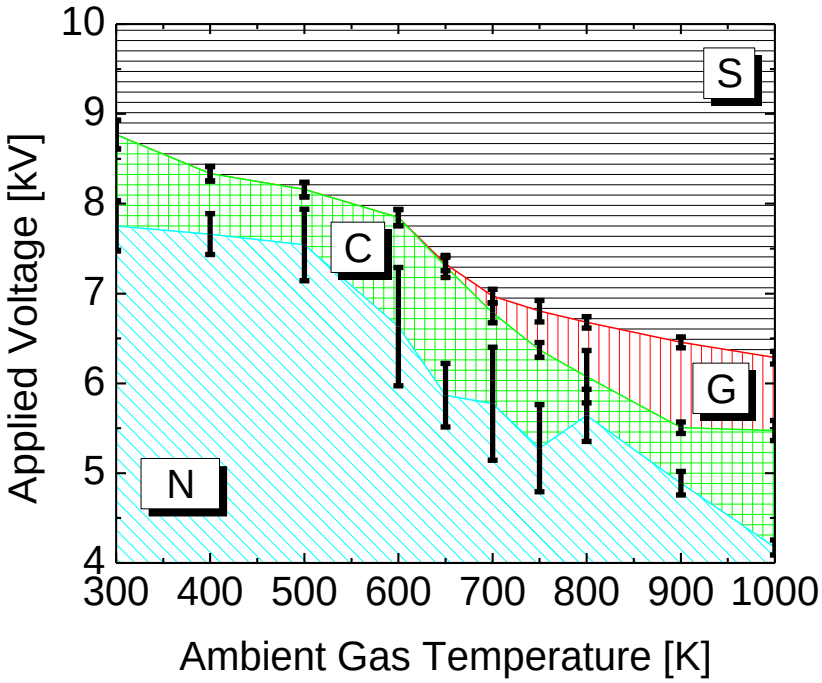

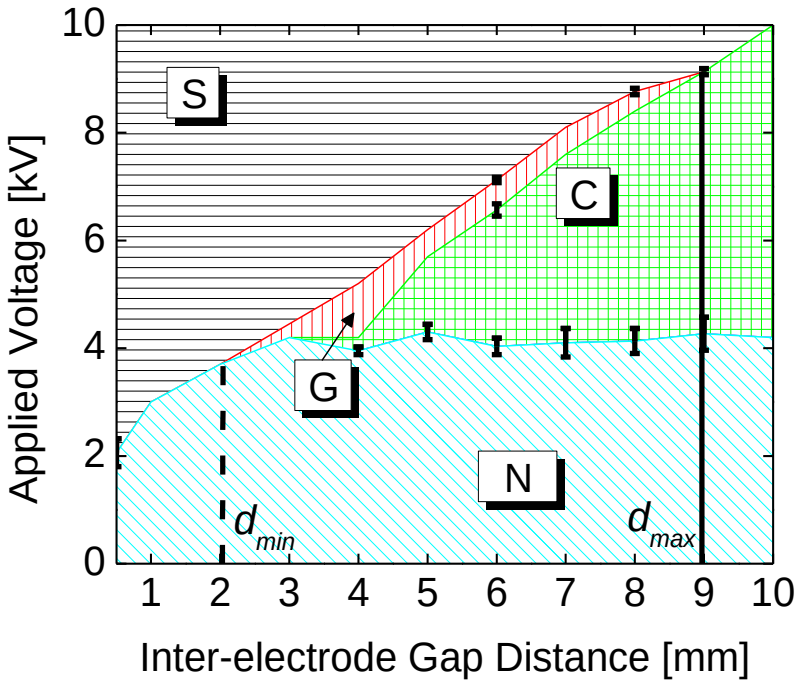

Carte des régimes selon la tension appliquée en fonction de la température du gaz ambiant.

f = 30 kHz, d = 5 mm, u = 1.6 m/s.

Carte des régimes selon la tension appliquée en fonction de la température du gaz ambiant.

T_0 = 1000 K, f = 30 kHz, u = 1.6 m/s.

Transition entre les régimes glow et spark NRP

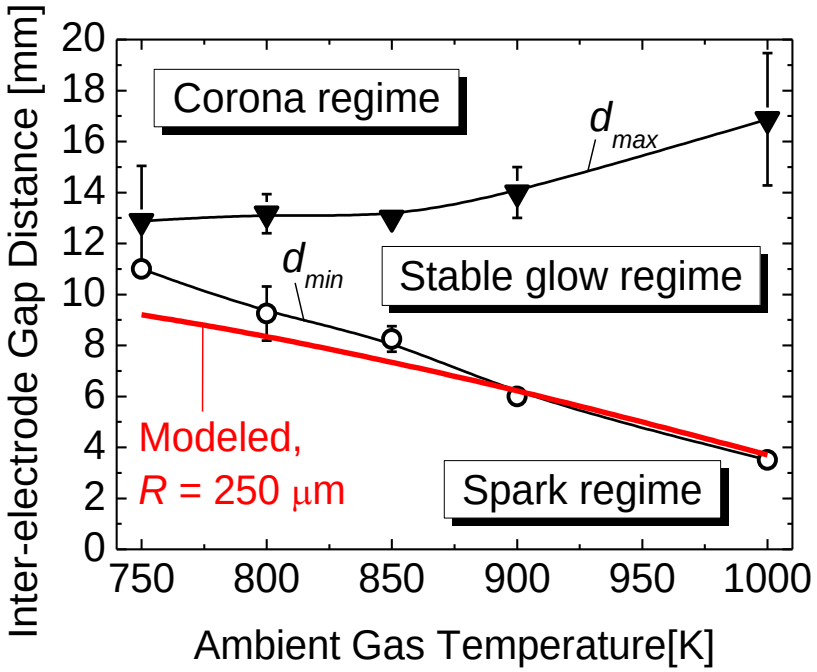

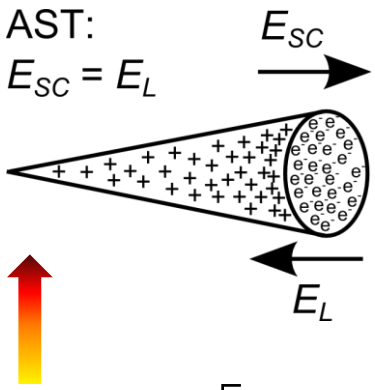

E_L: Laplacian field

E_{SC}: space-charge field

$$\underbrace{\alpha_{AST}^2 K}_{\text{Avalanche-to-Streamer transtion}} \underbrace{R \ln\left[\frac{1+\eta_0(d)}{1-\eta_0(d)}\right]}_{\text{Electrode geometry}} \leq \underbrace{\left(\frac{E}{N}\right)_{GS}}_{\text{Thermal ionization instability}} N d + \underbrace{V_{cf}}_{\text{Cathode fall voltage}}$$

$$T_g \uparrow \rightarrow E/N \uparrow \rightarrow n_e \uparrow \rightarrow P \uparrow \rightarrow T_g \uparrow$$

Domaine de la distance inter-électrode d permettant le régime NRP glow, et d_{min} modélisé

Pai et al, JAP 2010

Choisir tension appliquée et géométrie des électrodes :

- E_L au point suffisant pour l'AST
- E_{SC} dans le gap inférieure à $(E/N)_{GS}$

Régimes des décharges à champ « moyenne »

Gas	T_g [K]	Pulse width [ns]	PRF [kHz]	Discharge	n_e [cm^{-3}]	Method	Reference
Air 1 atm	2000	10	100	Glow	1.7×10^{12} max. 7×10^{11} min.	Current-voltage	Kruger *et al.* 2002
H_2 0.2 – 0.4 atm	300	10	12	Glow	2.5×10^{12} max. 4.5×10^{10} min.	CARS, current	Muller *et al.* 2011
Air 1 atm	300	10	5	DBD	1.4×10^{13} av.	Current-voltage	Walsh *et al.* 2007
Air 1 atm	300	12 – 13	1	DBD	2.3×10^{12} av.	Current-voltage	Shao *et al.* 2008
He 1 atm	300	90	1	DBD	8×10^{12} max.	mm-wave interferometry	Lu *et al.* 2008
Air 1 atm	1000	10	30	Spark	3×10^{15} max.	Current-voltage	Pai *et al.* 2010a
Air 1 atm	300	75	0.1	Spark	10^{15} max.	Laser Thomson scattering	Grisch *et al.* 2009
Ar-Ne 1 atm	300	30	10	Microplasma	6×10^{18} max.	Stark/atomic line ratios	Zhu *et al.* 2012
Air 1 atm	350	10	8	Microplasma	1×10^{19} max	Stark	Orrière *et al.* 2018
Air + 1,6% H_2 1 atm	300	10	0,05	Thermal spark	4×10^{19} max	Stark	Minesi *et al.* 2020
Air	300	20	0,01	Thermal spark	9×10^{18} max	Stark	Lo *et al.* 2017

NRP Glow

Diane Rusterholtz, PhD Thesis, Ecole Centrale Paris, 2012

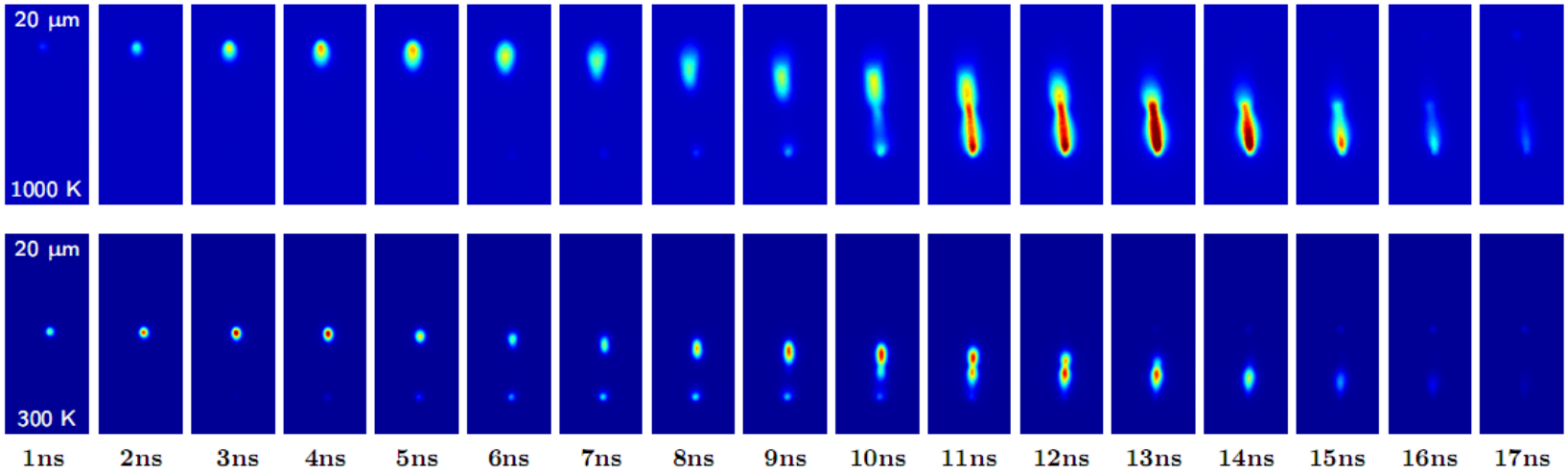

Figure 5.24: Images integrated during 2 ns of a glow discharge for (top) $T_g = 1000$ K, $d = 4.0$ mm, and $V_p = 4.0$ kV and (bottom) $T_g = 300$ K, $d = 2.5$ mm, and $V_p = 4.7$ kV (bottom). Images are averaged over several discharges. $R = 20$ µm, $l = 3.5$ mm, $PRF = 10$ kHz, and $v \approx 1.5$ m.s^{-1}. Intensity $I = 150$ (top) and $I = 250$ (bottom).

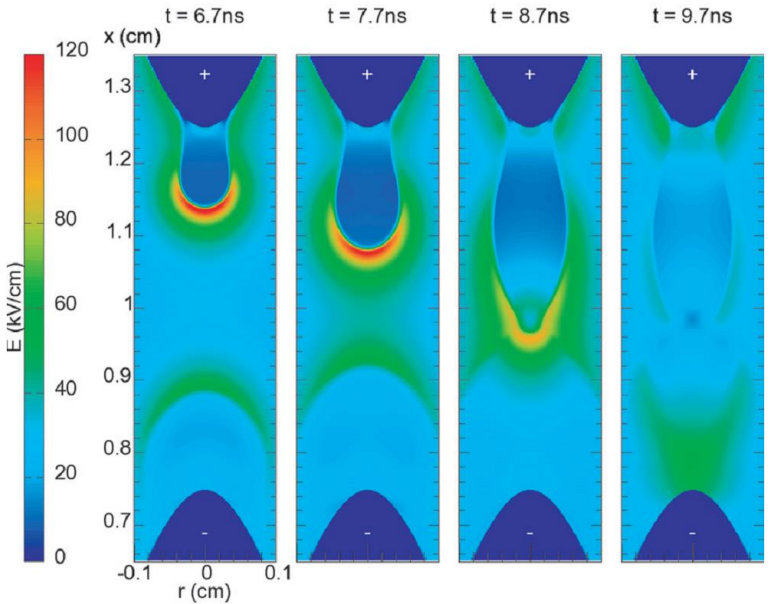

Tholin & Bourdon, PSST 2013

Décharge de surface

Stepanyan et al, PSST 2014

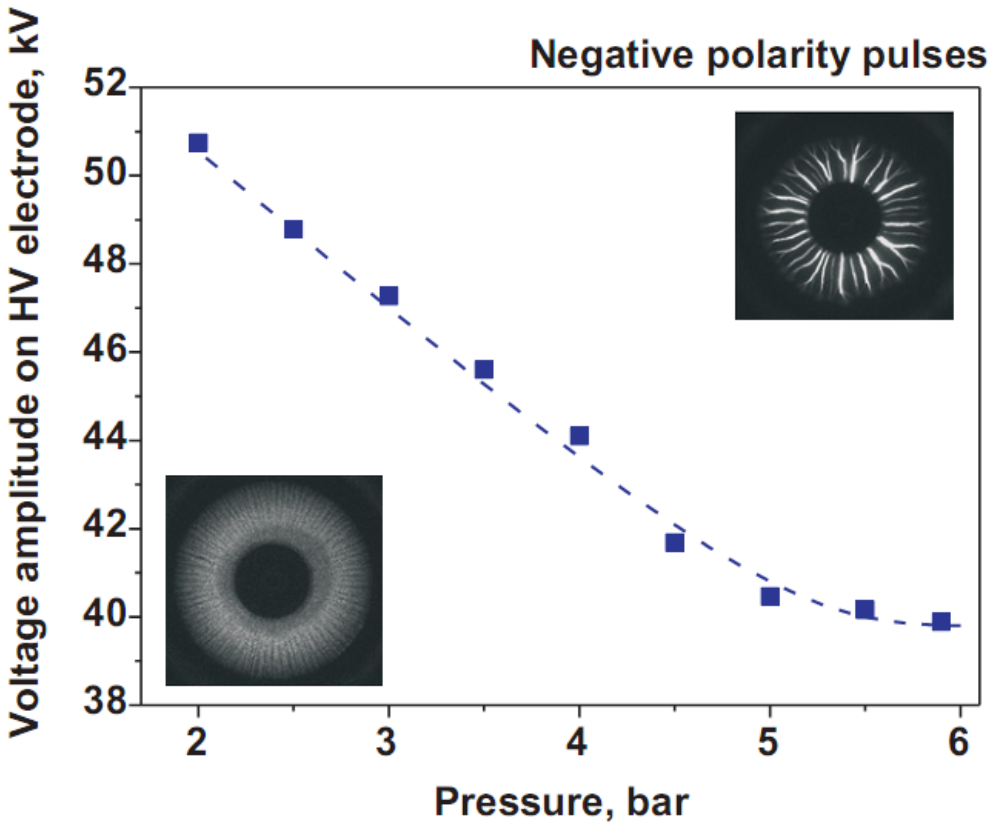

Figure 6. Curve separating regions of quasi-uniform diffusive (under the curve) and filamentary (above the curve) discharges as a function of pressure and applied voltage; negative polarity of the applied pulses; synthetic air.

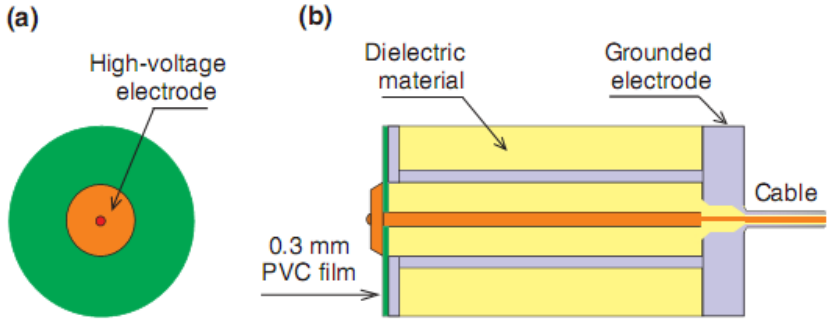

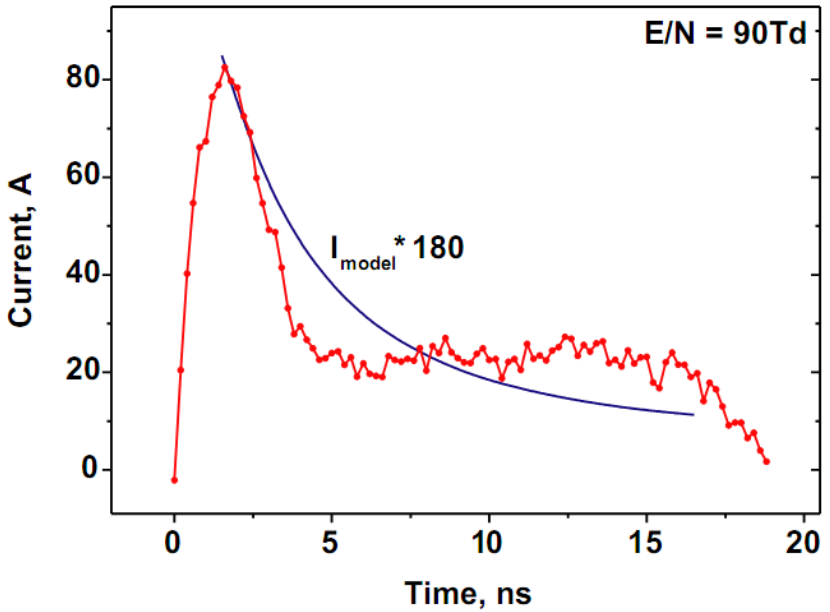

Figure 14. Discharge current as a function of time. The curve with points corresponds to the experimental curve, the solid curve corresponds to calculations at $E/N = 90$ Td, $N_e^0 = 2.5 \times 10^{15}$ cm^{-3}, $R_0 = 0.1$ mm; air, $P = 3$ bar, $T = 300$ K. The number of streamers was taken equal to $Z = 180$.

Décharge de surface

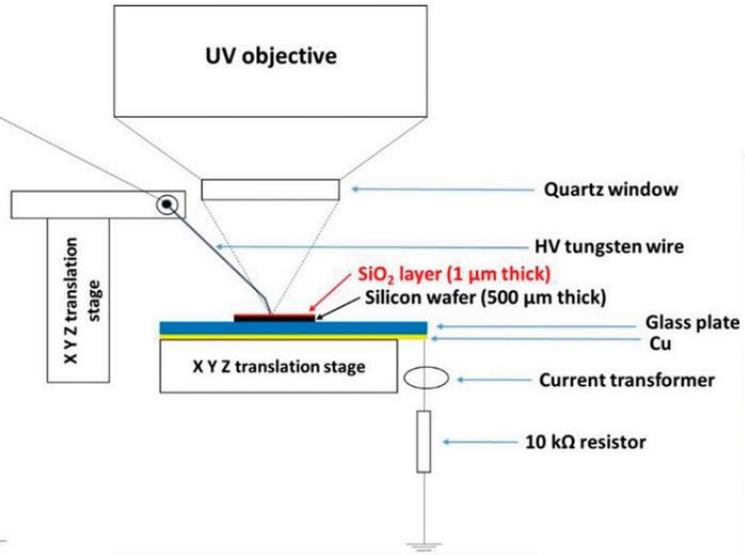

Darny et al, PSST 2020

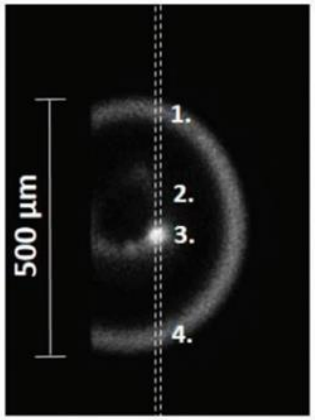

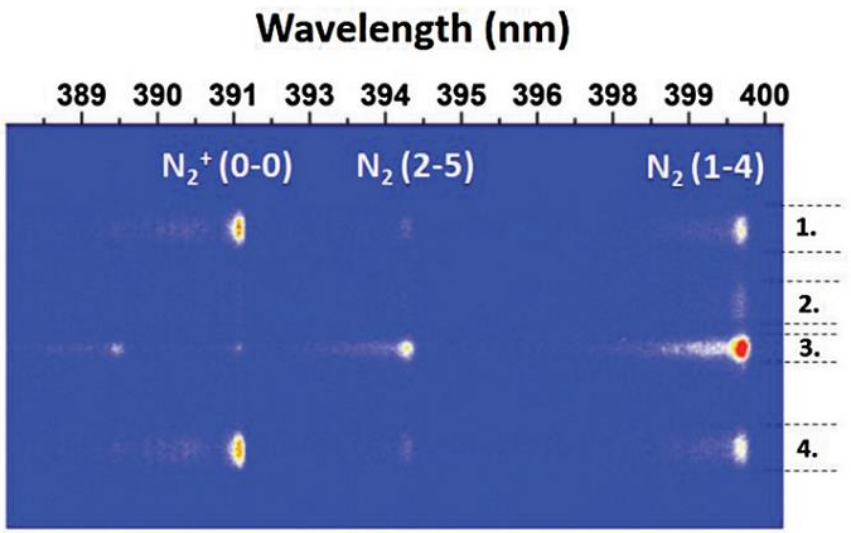

Verre

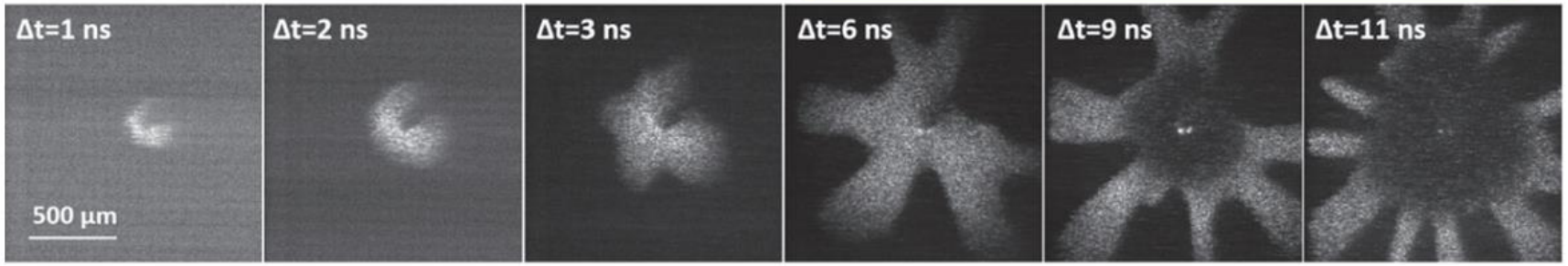

Si-SiO_2

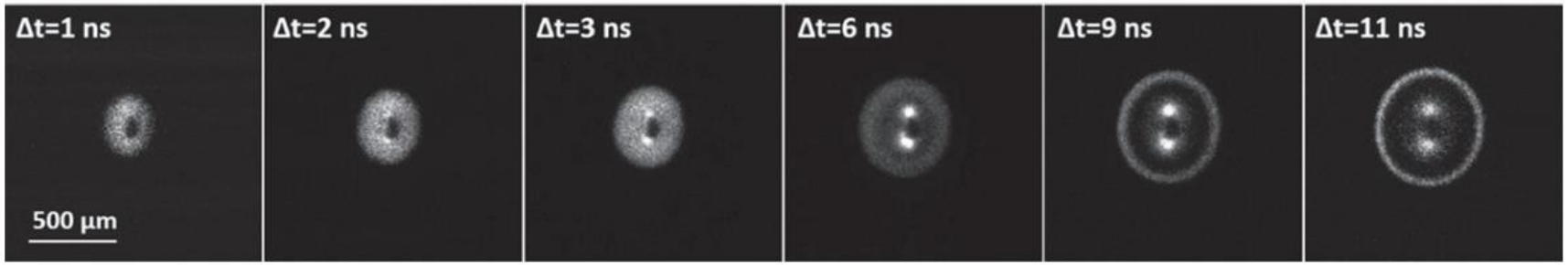

NRP Microplasma (cousin du NRP spark)

Thomas Orrière, PhD Thesis, Université de Poitiers, 2018

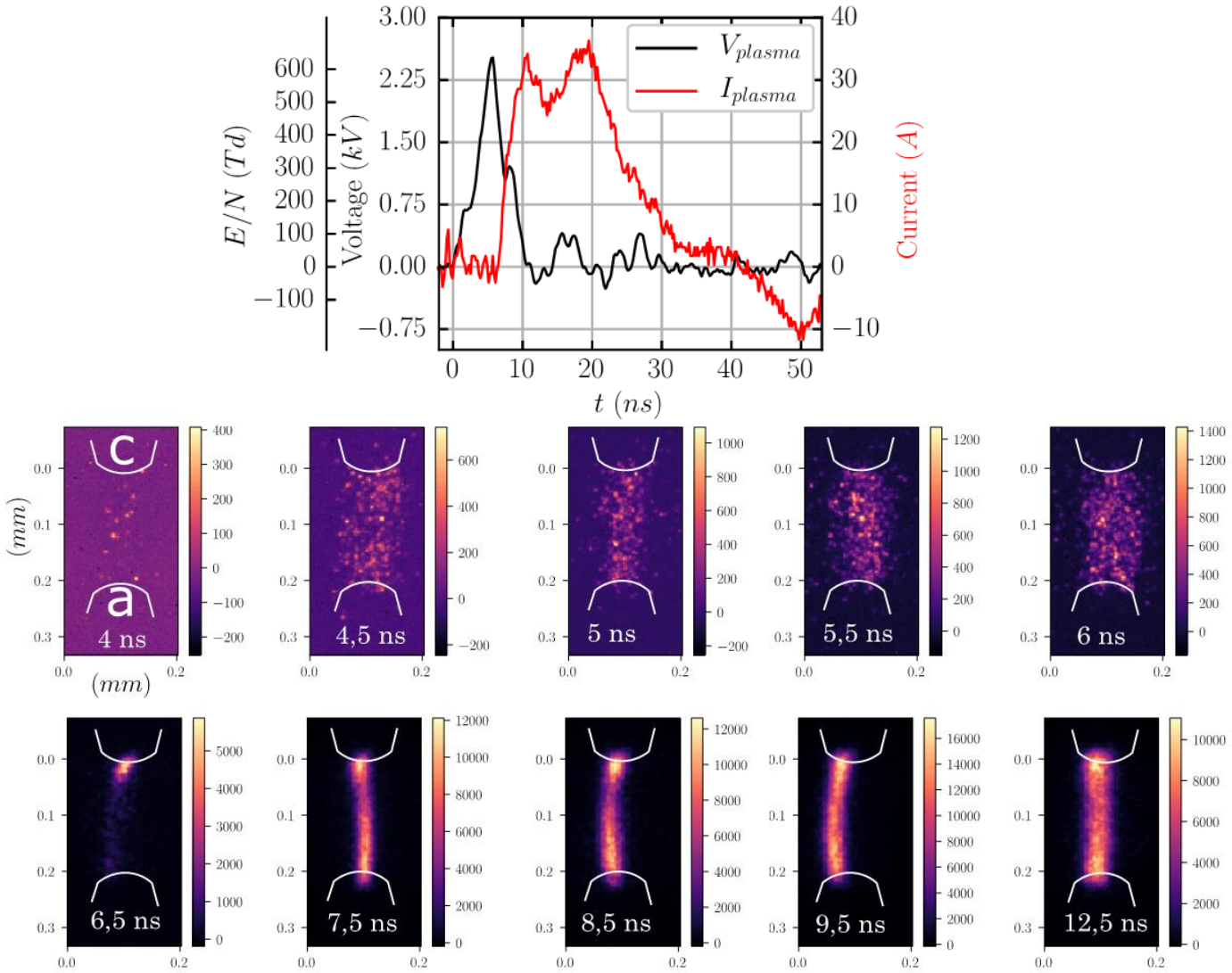

Figure 41:Imagerie instantanée de plusieurs décharges pour 4 ns $\leq t \leq$ 12,5 ns avec les conditions expérimentales de la figure 39 (d_{gap} = 200 µm, F_{NRP} = 8 kHz) . Le gain est resté constant et t_{exp} = 3 ns sur tous les pas de temps. Aucune émission n'est observée à t = 3,5 ns.

Thermal spark

Electrode polarities	Cathode–anode
Interelectrode gap	0.9 mm
Deposited energy	2.5–3.5 mJ per pulse
Amplitude of	Cathode: −5 kV
incident pulse	Anode: +3.5 kV
Pressure	58 mbar–1 bar
Gas	Ambient air

Minesi et al, PSST 2020

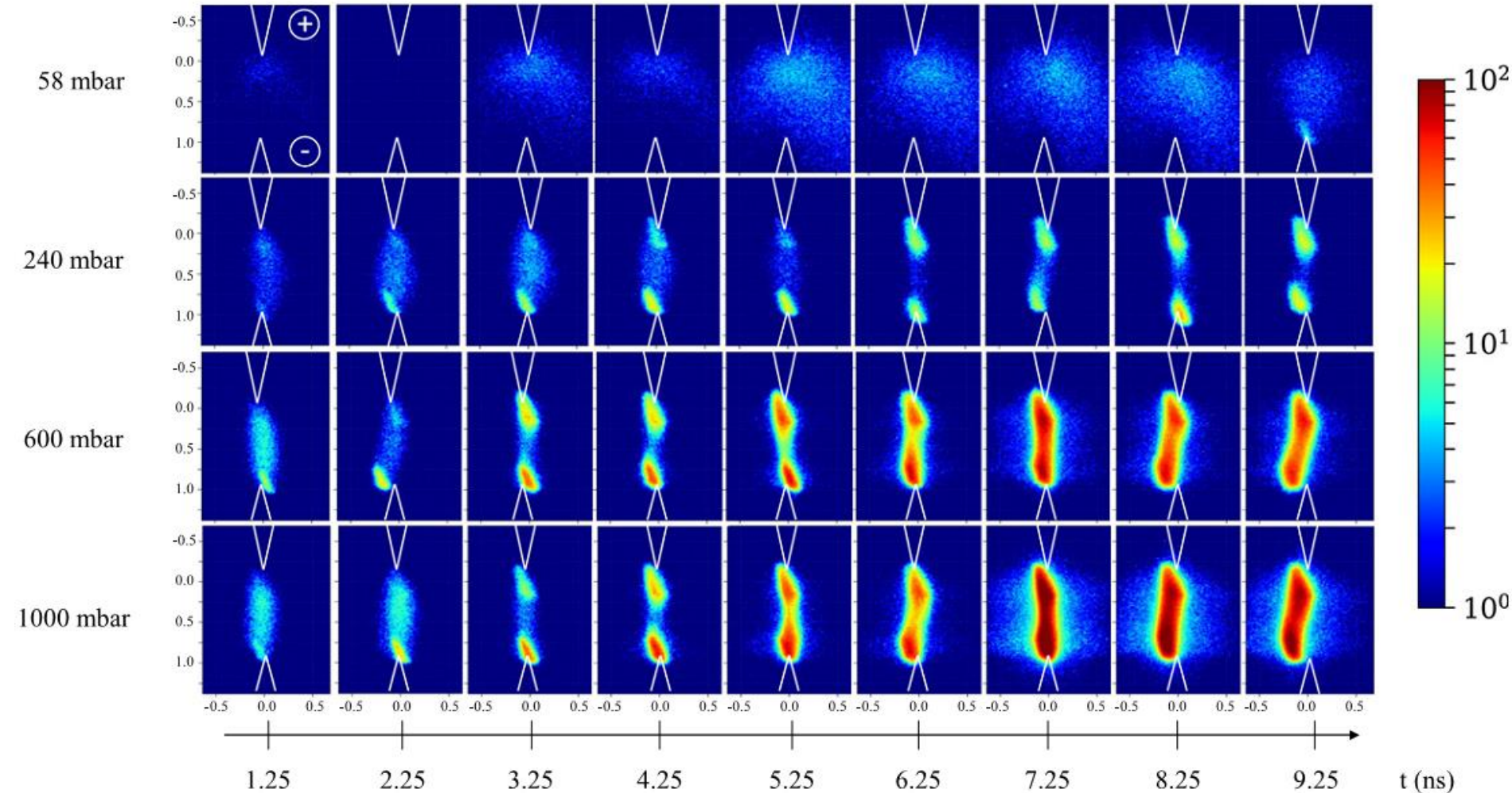

Thermal spark ?

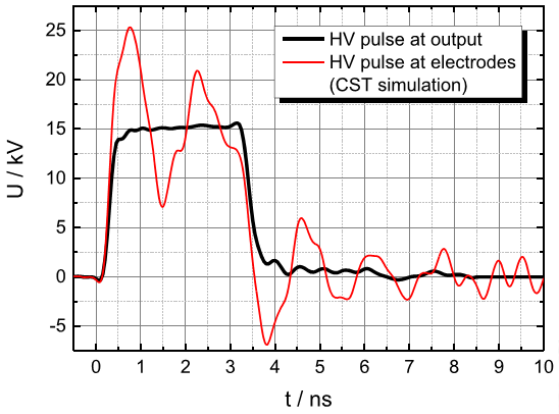

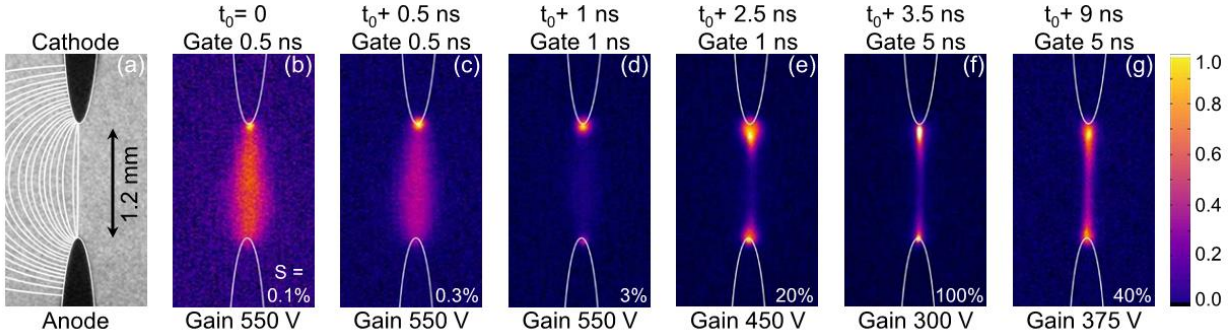

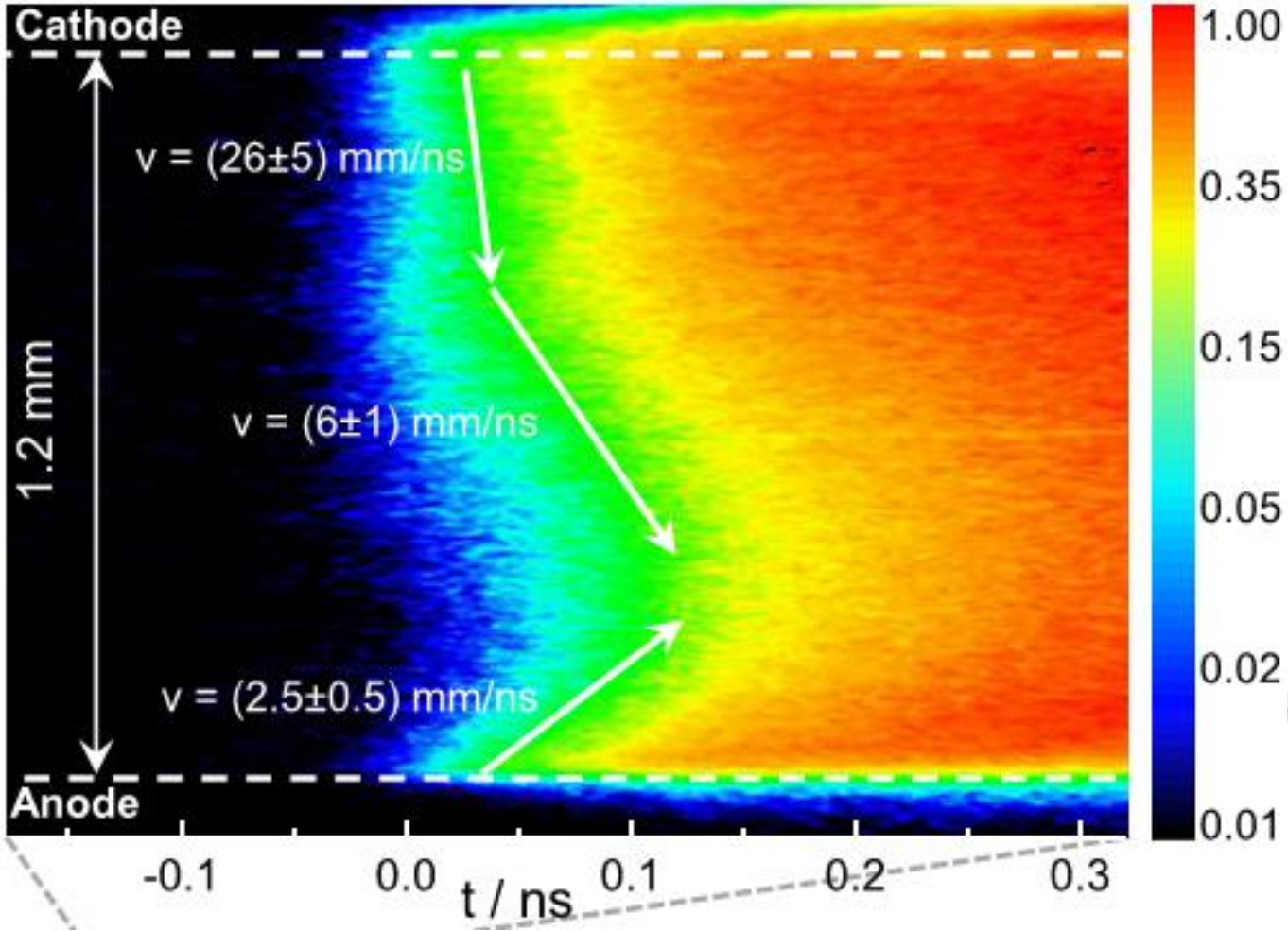

Hoft et al, PSST 2020

Fast Ionization Waves

Préionisation par électrons « runaway » → Décharge diffuse

Starikovskaia et al, J Phys D, 1998

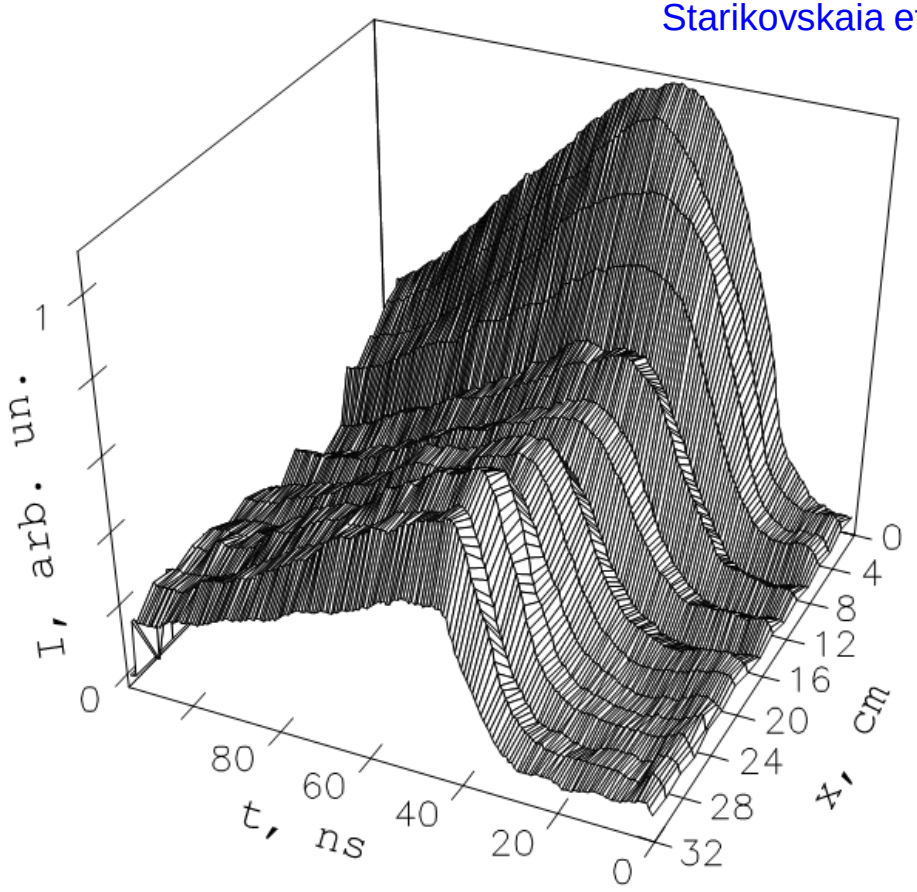

Figure 2. The time dependence of the emission intensity *I* for various distances from the low-voltage electrode along the vertical discharge cell axis. $U = -14.8$ kV and $P = 8.3$ Torr.

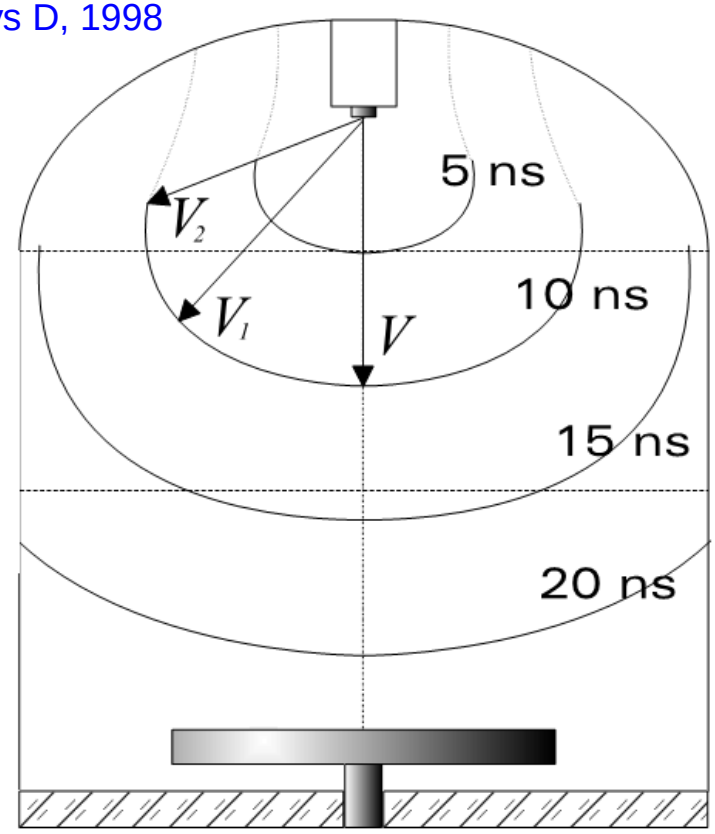

Figure 3. A schematic image of the propagation of the FIW front. $U = -14.4$ kV, $P = 0.4$ Torr, $|V| = 1.4$ cm s^{-1}, $|V_1| = 1.4$ cm s^{-1} and $|V_2| = 1.2$ cm s^{-1}. The figures near the curves denote the time elapsed from the start of the ionization wave.

Fast Ionization Waves à 1 atm

Brisset et al, PSST 2019

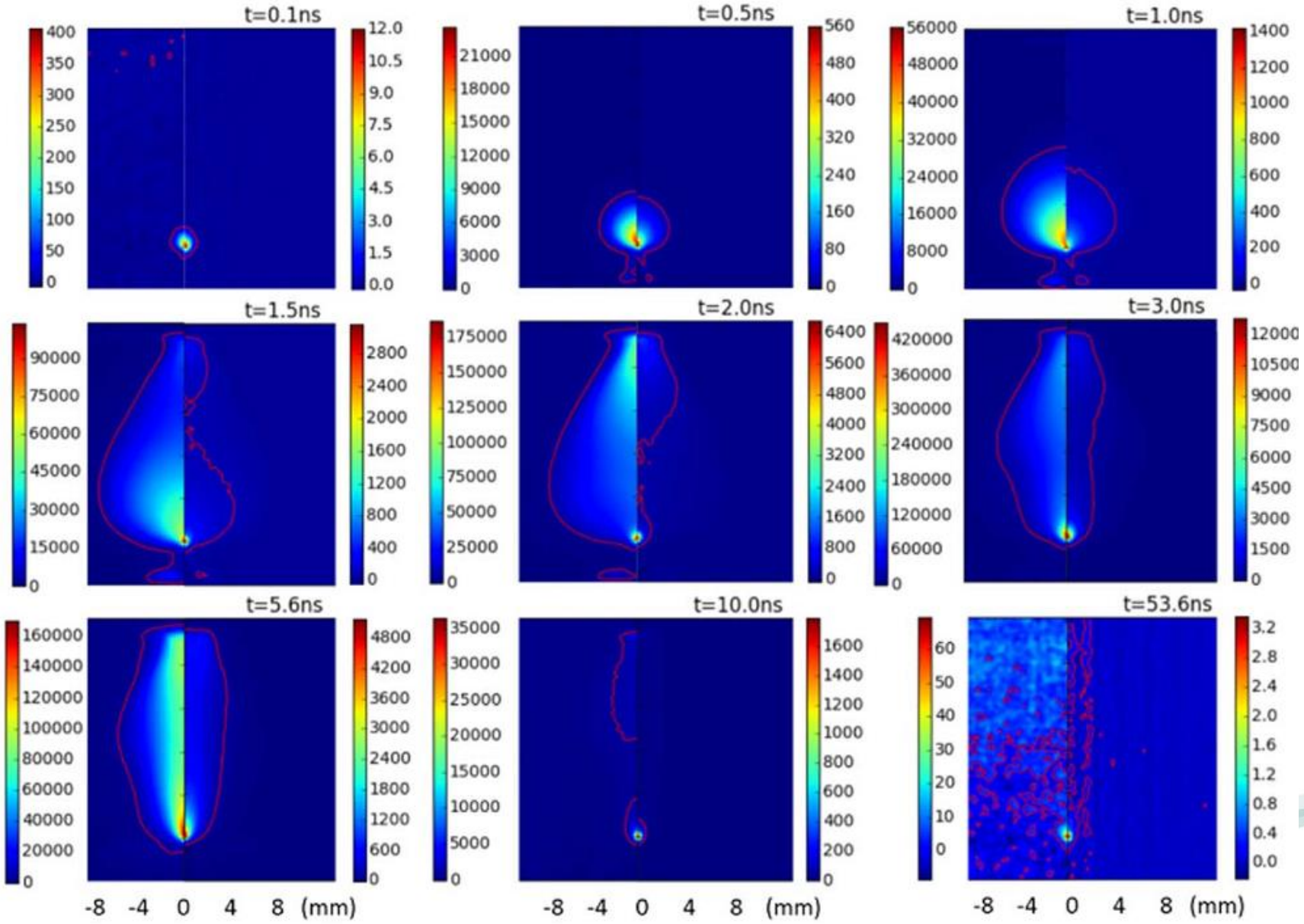

Fast Ionization Waves à 1 atm

Brisset et al, PSST 2019

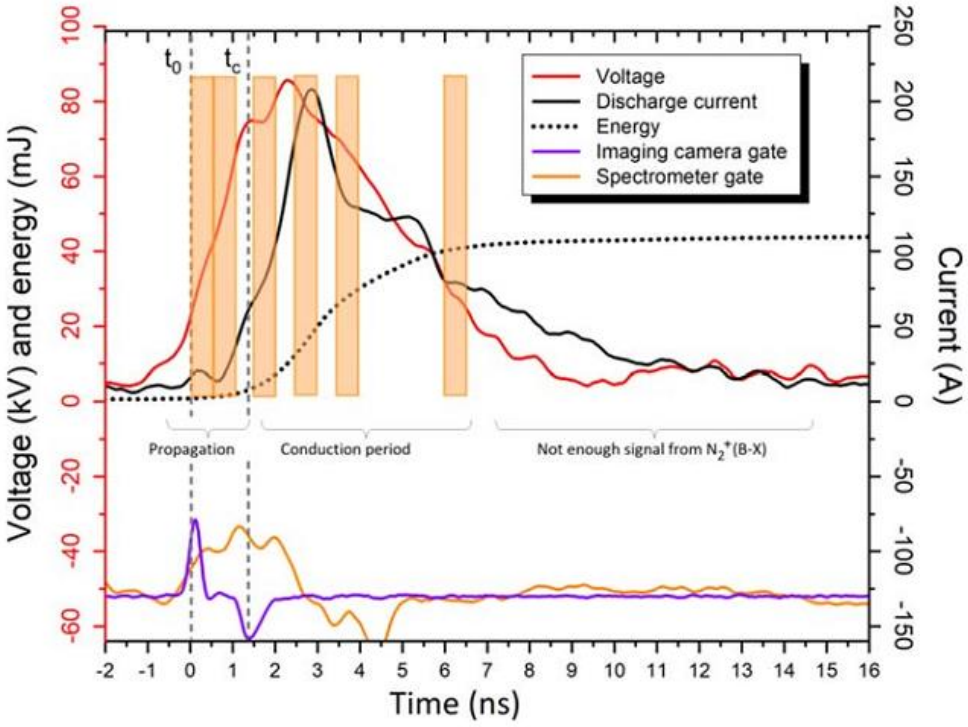

Chng et al, PSST 2019

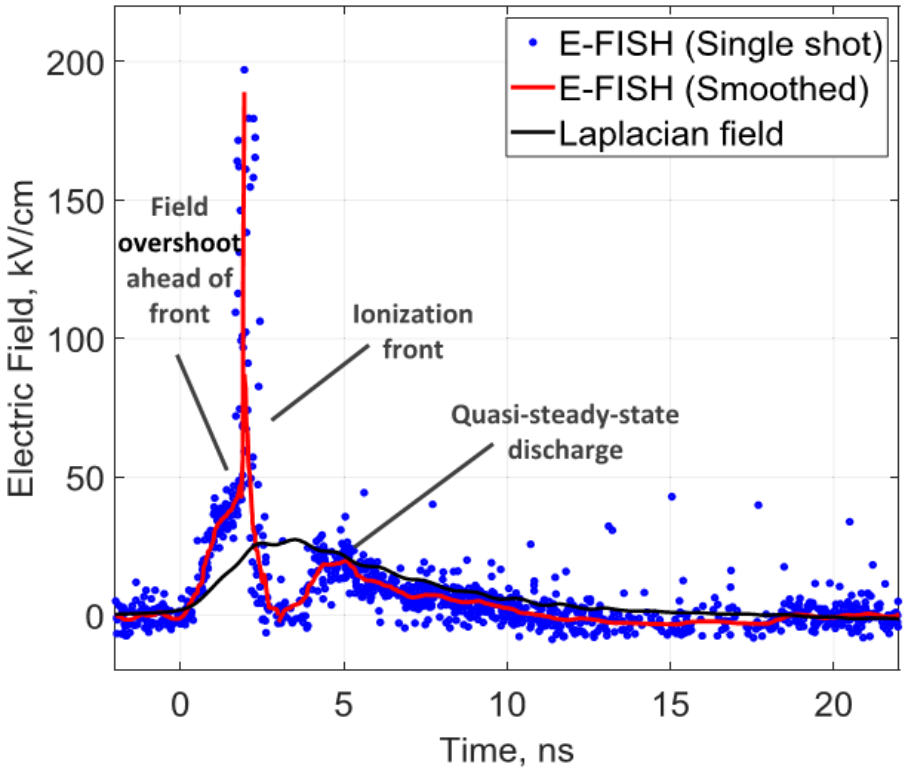

E/N jusqu'à 3000 Td par OES

Rappel

- Décharges impulsionnelles comme réponse impulse du gaz à un champ électrique → Analyse par temps caractéristiques

$$\tau_\sigma = \varepsilon_0 / \sigma$$

$$\tau_u = 1 / v_m \delta_l$$

$$\tau = 1 / kN$$

- Traitement simplifié des streamers comme nuages de charge

$$E' = \frac{1}{4\pi\varepsilon_0} \frac{eN_e}{R^2}$$

$$dR/dt = \sqrt{D / 2t}$$

$$dR/dt = \mu_e E'$$

- Critère de Raether-Meek

$$\alpha x_{crit} \approx 18$$

Merci de votre attention !

Exemple faiblement ionisé dans le CO

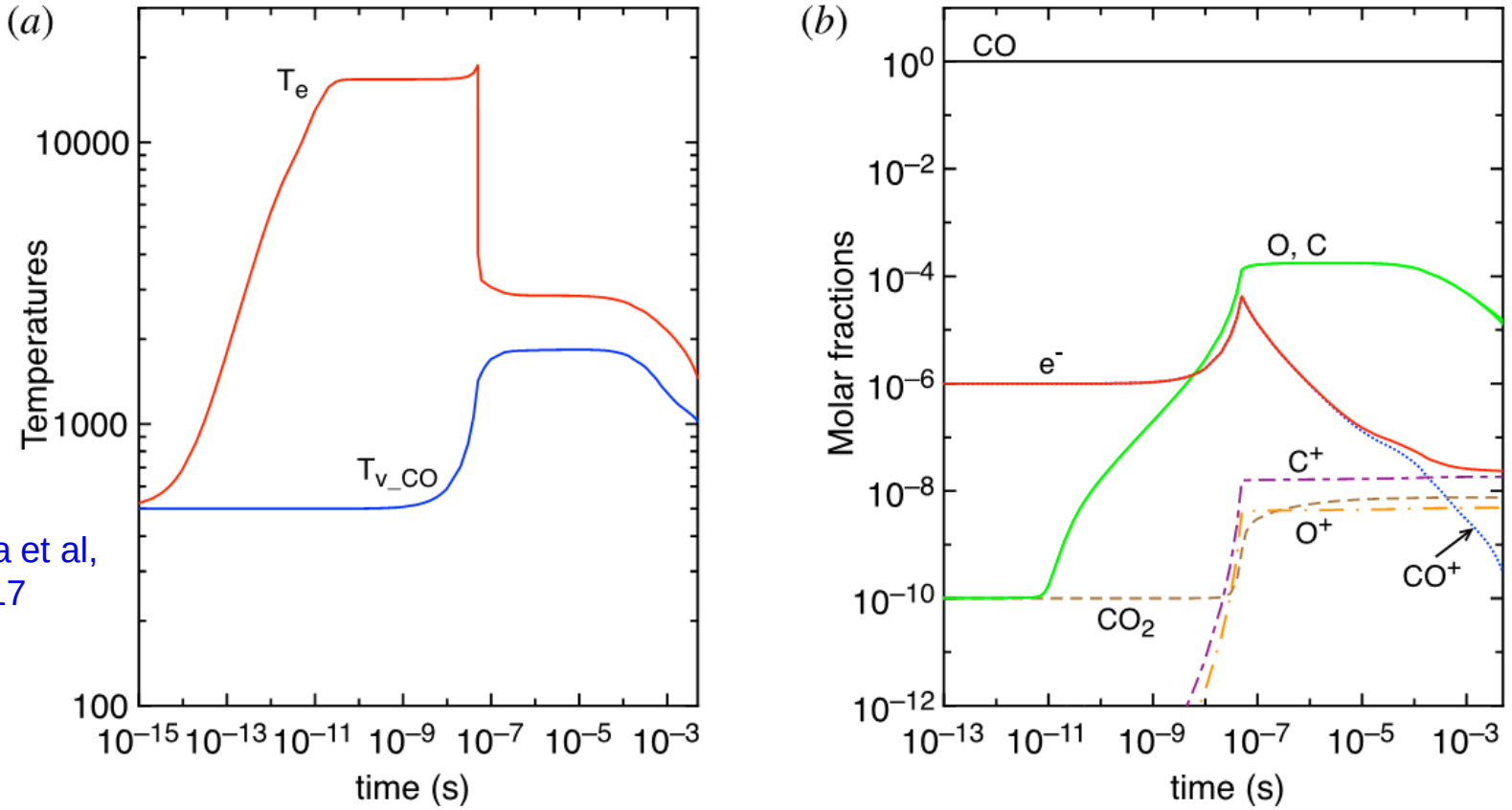

Pietanza et al, JPP 2017

FIGURE 6. (*a*) Temperature and (*b*) molar fraction time evolution in case study 2 ($T_{gas} = 500$ K, $p = 1$ atm, E/N = 130 Td, $\tau_{pulse} = 50$ ns, $\tau_{afterglow} = 4$ ms).

τ_{EEDF}	τ_{e-V}	τ_{V-V}	$\tau_{V-T(CO)}$	$\tau_{V-T(C,O)}$
5.57×10^{-12} s	1.30×10^{-7} s	4.37×10^{-8} s	5.56×10^{-2} s	3.50×10^{-7} s

TABLE 3. Characteristic times evaluated at the end of the pulse ($\tau_{pulse} = 50$ ns) when the electron density is approximately 2×10^{15} cm^{-3}.

Exemple faiblement ionisé dans le CO

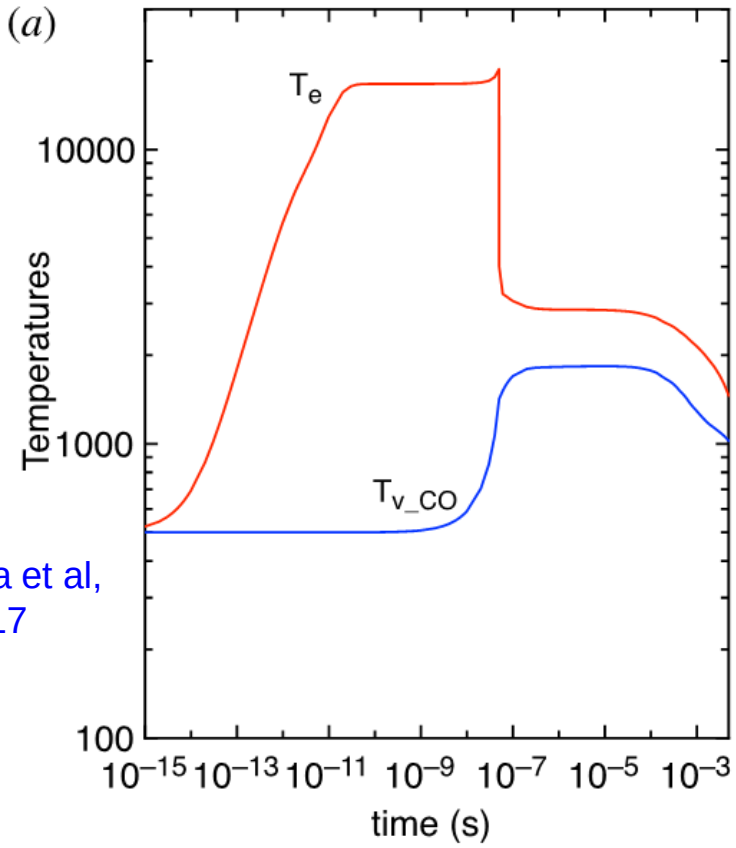

Pietanza et al, JPP 2017

$$\nu_m = N\sigma_m\sqrt{8k_BT_e/\pi m_e} = 1.42 \text{ THz}$$

$$\delta_l = 0.039$$

$$\tau_u = 1/\nu_m\delta_l = 1.8\times10^{-11} \text{ s}$$

FIGURE 6. (*a*) Temperature and (*b*) molar fraction time evolution in case study 2 (T_{gas} = 500 K, p = 1 atm, E/N = 130 Td, τ_{pulse} = 50 ns, $\tau_{afterglow}$ = 4 ms).

τ_{EEDF}	τ_{e-V}	τ_{V-V}	$\tau_{V-T(CO)}$	$\tau_{V-T(C,O)}$
5.57×10^{-12} s	1.30×10^{-7} s	4.37×10^{-8} s	5.56×10^{-2} s	3.50×10^{-7} s

TABLE 3. Characteristic times evaluated at the end of the pulse (τ_{pulse} = 50 ns) when the electron density is approximately 2×10^{15} cm^{-3}.

Exemple faiblement ionisé dans le CO

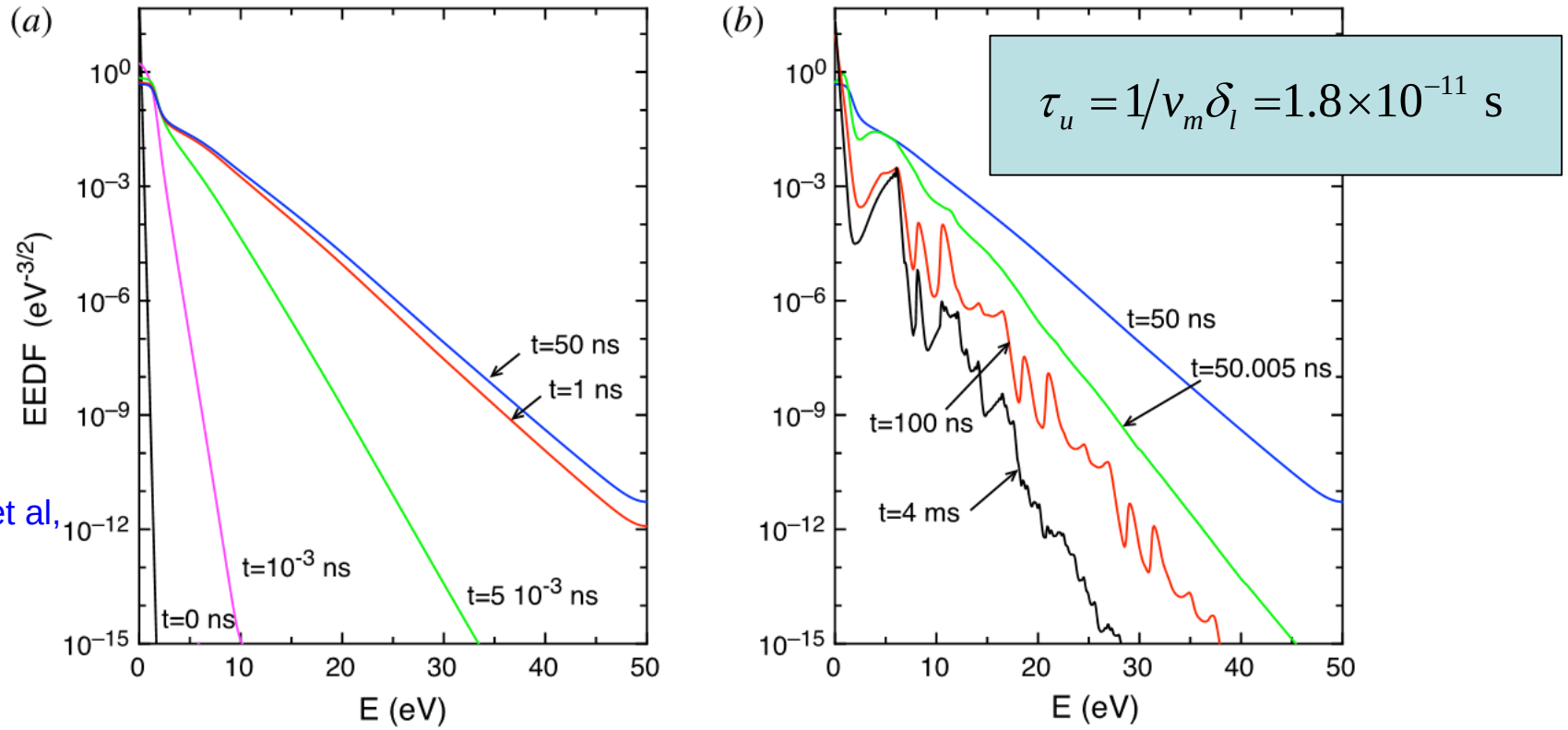

Pietanza et al, JPP 2017

FIGURE 8. Electron energy distribution function in (*a*) discharge and (*b*) post-discharge conditions for case study 1 (T_{gas} = 500 K, p = 1 atm, E/N = 130 Td, τ_{pulse} = 50 ns, $\tau_{afterglow}$ = 4 ms).

τ_{EEDF}	τ_{e-V}	τ_{V-V}	$\tau_{V-T(CO)}$	$\tau_{V-T(C,O)}$
5.57×10^{-12} s	1.30×10^{-7} s	4.37×10^{-8} s	5.56×10^{-2} s	3.50×10^{-7} s

TABLE 3. Characteristic times evaluated at the end of the pulse (τ_{pulse} = 50 ns) when the electron density is approximately 2×10^{15} cm^{-3}.

Champ électrique

Temps de Maxwell est pour une valeur de n_e donnée

Temps d'écrantage tenant compte l'ionisation :

$$\tau_{is} = \frac{\ln\left(1+\frac{\alpha\varepsilon_0 E_0}{en_0}\right)}{\alpha\mu_0 E_0}$$

Teunissen et al, J Phys D 2014

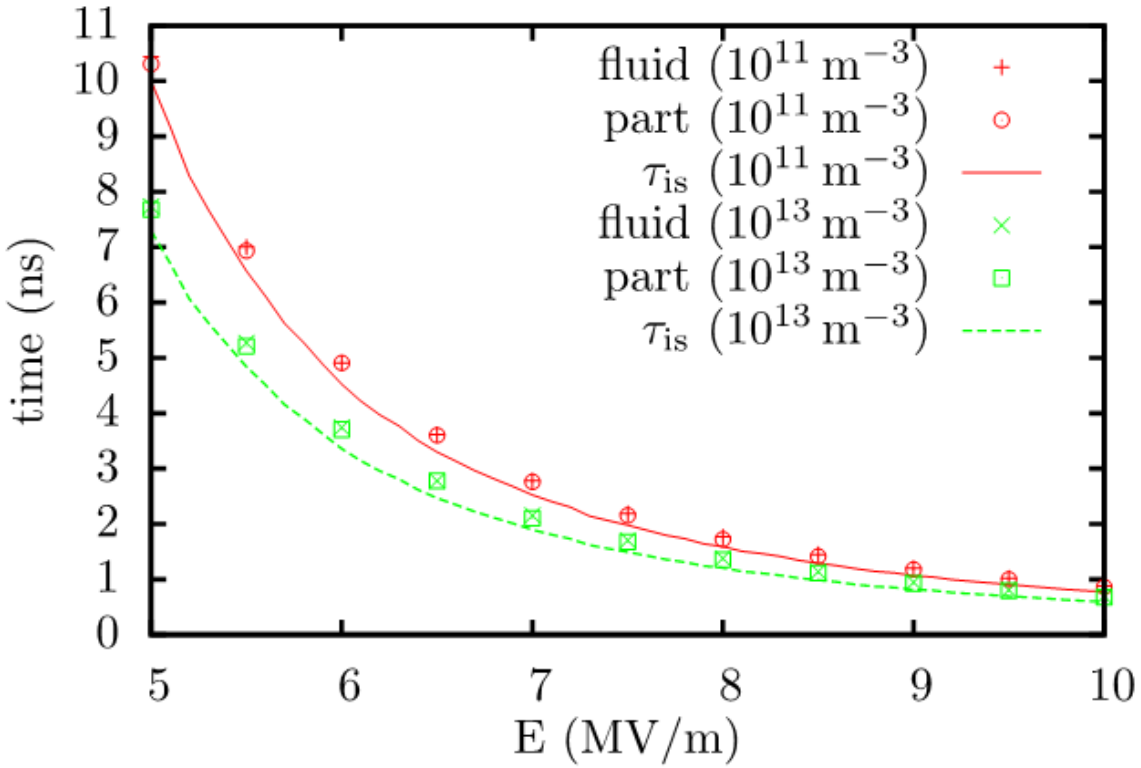

Figure 2. The ionization screening time versus the applied electric field, for two initial plasma densities (10^{11} and 10^{13}). Results are shown for a 1D fluid model, a 1D particle model and equation (6), for N_2 at 1 bar.

Transition entre les régimes glow et spark NRP

Diane Rusterholtz, PhD Thesis, Ecole Centrale Paris, 2012

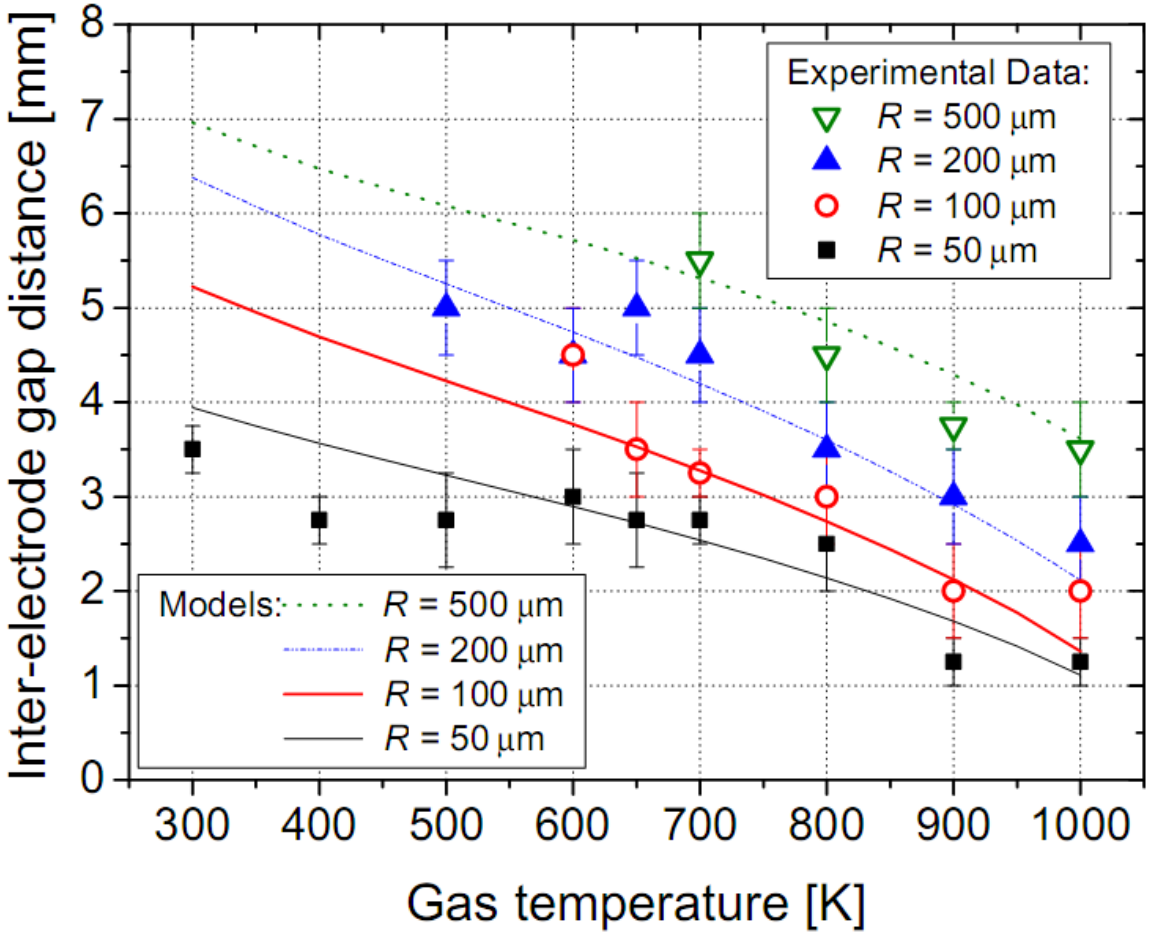

(a) Minimum distance d_{min}